Integrating Gravimetry Data with Thermal Infra-red Data from Satellites to Improve Efficiency of Operational Irrigation Advisory in South Asia

Indira Bose

A thesis

submitted in partial fulfillment of the

requirements for the degree of

Master of Science in Civil Engineering

University of Washington

2020

Reading Committee:

Faisal Hossain

Rebecca B. Neumann

Program Authorized to Offer Degree:

Civil and Environmental Engineering

University of Washington

Abstract

Integrating Gravimetry Data with Thermal Infra-red Data from Satellites to Improve Efficiency of Operational Irrigation Advisory in South Asia

Indira Bose

Chair of the Supervisory Committee:
Professor Faisal Hossain
Civil and Environmental Engineering

The rapid decline of groundwater resources in South Asia due to excessive irrigation during dry season requires awareness of optimal on-field water allocation requirements that is now being provided to farmer cellphones through an operational Irrigation Advisory System (IAS). To minimize the cost of sending such irrigation advisory texts to farmers while maximizing impact of IAS on groundwater sustainability we integrated Gravity Recovery and Climate Experiment (GRACE) data with Landsat Thermal Infrared (TIR) Imagery to target regions in greater need of the IAS service. We demonstrated the concept of an improved IAS with the integration of GRACE and Landsat TIR data over eight irrigation districts of the Ganges and Indus basins. The Surface Energy Balance Algorithm for Land (SEBAL) was used to monitor on-field water consumption (evapotranspiration-ET) over cropped areas using Landsat TIR data at plot-scale

spatial resolution. Comparison of SEBAL ET with crop water demand from Penman-Monteith (FAO56) technique quantified the extent of over-irrigation at the plot scale and provided a tangible pathway to micro-target the IAS service only to farmers with the largest groundwater use footprint, thereby maximizing the efficiency of the IAS service. Our results suggested that an operational IAS that integrates GRACE and Landsat TIR data on average can save about 85% (80 million m^3) of groundwater per dry season for irrigation districts of Northern India and 87% (or 150 million m^3) per year for irrigation districts of Eastern Pakistan. Our proposed enhanced IAS will also allow continuous monitoring of farmer behavioral change in reducing over-irrigation and long-term impact on groundwater resources with need-based irrigation practices via follow up assessment of GRACE TWS (after dry season) and TIR data (during dry season).

TABLE OF CONTENTS

LIST OF FIGURES

ACKNOWLEDGEMENTS

I take this opportunity to express the sincerest gratitude to Professor Faisal Hossain for his supervision, mentorship, encouragement, and guidance throughout the research work. He showed a perfect example of both a researcher and an advisor and it has been my fortune and pleasure to work with him. I am also grateful to my committee member Professor Rebecca B. Neumann for her input and suggestions on this work.

I am also grateful to my peers Shahryar K. Ahmed, Hisham Eldardiry, Claire Beveridge and Nishan Biswas in the SASWE Research Group for their support and co-operation.

I am thankful to University of Washington Global Affairs and the Ivanhoe Foundation for their generous contributions that enabled meaningful stakeholder interaction. I am also thankful to the NASA Applied Sciences Program and National Science Foundation for supporting parts of the project. I gratefully acknowledge the consistent support and feedback provided by the Pakistan stakeholder agency – Pakistan Council of Research in Water Resources (PCRWR) as part of a long-standing Memorandum of Understanding with University of Washington for technical collaboration since 2015.

This acknowledgement is incomplete without the mention of my family members. I want to extend the greatest and deepest appreciations to my husband, parents and brother for their endless love, support, and encouragement throughout my life.

DEDICATION

This thesis is dedicated to my husband, Dr. Partha Saha; my parents, Tarun Kumar Bose and Bichitra Bose and my brother, Tanumoy Bose Sagar.

Chapter 1. INTRODUCTION

1.1 MOTIVATION

Groundwater, one of the most important freshwater resources, satisfies significant water demand required by irrigational (42%), domestic (36%), and industrial uses (27%) (Döll et al., 2012; Famiglietti, 2014; Taylor et al., 2013). It also sustains surface water systems during dry seasons, by maintaining a stable groundwater table worldwide. However, a growing population requires increased agricultural productivity. This consequently triggers a significant and often unsustainable extraction of groundwater storage around the world (Siebert et al., 2015). The evident correlation of groundwater depletion with extensive irrigation activity is very distinct in South Asian countries where the monsoon weather system dominates the precipitation regime. The monsoon is a system with prevailing winds along a certain direction. It brings in bountiful amounts of rain (wet phase) followed by a reversal in wind direction resulting in no precipitation (dry phase) (Ramage, 1971). Each phase lasts at least 4-5 months and the dry phase is markedly non-precipitating with low streamflow and dry soils. During the dry phase of the monsoon, irrigation activities for food production are sustained only from groundwater recharged by the rains from the previous wet season.

South, Southeast, and East Asia sustain extensive irrigation systems by relying entirely on groundwater pumped during the dry season from November to April (Hossain et al., 2017). Hence, the water and food security in South Asia is deeply rooted into groundwater resources of the transboundary aquifer system of Indus-Ganges-Brahmaputra-Meghna (IGBM) rivers with a net cropping area of 114 million ha (Malakar et al., 2020; Mukherjee et al., 2015). For South and East Asia, the total annual water withdrawal is roughly 1981 km^3, which is about 50 percent of world's

withdrawals (FAO, 2016). Agriculture requires around 82 percent of the total freshwater withdrawal in Asia, which is much higher than global agricultural water withdrawal (70 percent) (FAO, 2016). The highest water withdrawal in South Asia is reported in India comprising of about 10400 m^3/ha of irrigated land (FAO, 2016). As a result of this high groundwater withdrawals, South Asia today experiences rapid groundwater depletion; predominantly in North-West (Ganges Basin) and South-East (Bengal basin) India, upper Indus Basin in Pakistan and Meghna basin in Bangladesh (MacDonald et al., 2016). Such extensive withdrawal of groundwater jeopardizes the water sustainability for the millions of farmers in South-Asia.

In addition to the boom of groundwater-dependent irrigation, wastage of water by irrigating more than the crop water demand also contributes to this unsustainable groundwater depletion. For instance, the water requirements for rice in Punjab and Sindh Provinces of Pakistan are approximately 600 and 1400 millimeters, respectively; but the farmers routinely apply around 2200 mm resulting in a significant loss of groundwater, and an increase in fuel cost due to pumping from deeper layers (Hossain et al., 2017). Therefore, a proper management of groundwater resources for agricultural uses is critical for a sustainable balance between groundwater supply and demand to ensure food security in the coming decades for South Asia (Malakar et al., 2020; Rahman et al., 2020). A recent study by the Central Groundwater Board of India has reported that Western India is likely to run out of its groundwater in another 20 years (Singh, 2020).

Optimizing irrigation according to crop water need can play an important role in ensuring a more sustainable use of ground water. By ensuring that farmers pump groundwater during the dry season according to the demand for crop growth rather than the archaic wasteful practice of overirrigation, an Irrigation Advisory Service (IAS) should be able to minimize the current and rampant groundwater wastage.

1.2 IRRIGATION ADVISORY SERVICE (IAS)

An IAS service advises farmers on when and how to irrigate. There are different devices and tools that provide farmers with guidelines and instructions on how to determine the correct time and application depth of the irrigation (Smith and Munoz, 2002). There has already been anecdotal evidence that an operational IAS can save groundwater based on recent implementation in Indus basin since 2016 (http://www.pcrwr.gov.pk/advisory.php and http://www.pak-ias.org) and more recently in India (http://www.i-pani.com), and Bangladesh (http://pani.hmrcweb.com).

To conserve groundwater and improve crop yield, one of the well-known IAS services for Pakistan Council of Research in Water Resources (PCRWR; http://www.pcrwr.gov.pk/advisory.php and http://www.pak-ias.org) was developed by Sustainability, Satellites, Water, and Environment (SASWE) research group of University of Washington (UW) in August 2016 (Hossain et al., 2017). This IAS is coined as a "smart" irrigation service and was operationalized for advising farmers on how much and when to irrigate based on crop water demand or evapotranspiration (ET) and forecast of precipitation and weather conditions. A proxy measure of the reference evapotranspiration rate (ETo), the crop water requirement for a crop, was computed using a method from Allen et al., (1998) which is known as Penman-Monteith (FAO 56) method. This technique was basically an alteration of a well-known equation reported in Monteith and Unsworth (1990) using temperature, humidity, wind speed, and solar radiation as inputs. The model outputs are nowcasts and forecasts of the need of water for each week and precipitation as well. The input to the model is obtained from a Global Numerical Weather Prediction (NWP) modeling system known as the Global Forecast System (GFS). The nowcast weather variables from GFS produce nowcast of crop water demand, precipitation, and other farming-relevant conditions such as humidity, windspeed and temperature. Similarly, the

forecast weather variables from GFS help produce forecast of the same variables. Lysimeter-based ET data were used by PCRWR to validate the nowcast inputs to indicate that the FAO56 based crop water demand (forecast and nowcast) was skillful enough to be used in IAS for farmers.

In this operationalized IAS, when supply (rainfall/recent irrigation) exceeds crop water demand, the farmers get advisory on their cellphones to skip or reduce irrigation. Similarly, when crop demand exceeds the supply, the farmers get the advisory to apply or increase irrigation. Such an IAS has also been successfully piloted over Kanpur in India under the name of Provision for Advisory on Necessary Irrigation (PANI) (http://www.i-pani.com). PANI was launched at the start of the winter wheat season of October 2018 and irrigation and weather advisory services were provided to farmers until harvest in March 2019. After harvest, the survey reported that out of the 150 farmers, 69 (57.4 percent) provided valuable feedback on the effectiveness of PANI (USAID Agrilinks, 2020). Most recently, the IAS has seen expansion to Bangladesh in 2019 on a pilot scale with 165 farmers (http://pani.hmrcweb.com). Starting with 700 farmers in Pakistan in 2016, tens of thousands of farmers are now experiencing the services of IAS in these monsoon-affected South Asian nations that are known to waste groundwater during the dry season when food production is critical.

According to a survey of randomly selected farmers carried out by PCRWR, it is speculated that the IAS can potentially save about 2.5 km^3 of groundwater a year per 100,000 farmers in Pakistan (IAS, 2018). This is equivalent to 40% potential savings in irrigation water. In recent years, IAS had positive impacts on increase in yield of wheat in Pakistan and India up to 500 kg/ha with 80%, 85% and 78% usage rate by farmers in Pakistan, India, and Bangladesh, respectively (IAS, 2018). Many other countries have also adopted crop water demand-based irrigation advisory

such as IAS. Examples are Castilla-La Mancha in Spain, Baixo Acaraú irrigation district in Brazil, and Australia (Car et al., 2012; Corcoles et al., 2016; Ortega et al., 2005).

Despite all the benefits of IAS, there is always room for improvement as IAS is a public service with an operational cost. In South Asian countries, this cost is maintained by governments, and therefore only a finite fraction of farmers can receive this service. These countries are not yet ready for a viable and universal service that is accessible to every single of the 130 million of farmers (Dixon et. al., 2001). So one area of improvement for IAS is to optimize the targeting of the service exclusively to regions and farmers where groundwater consumption for irrigation needs to be more urgently managed so that the overall impact on sustainability is larger for the same limited service.

1.3 Research Questions

The objective of this study is to improve the existing IAS by integrating Gravity Recovery and Climate Experiment (GRACE) Total Water Storage (TWS) anomaly data with Thermal Infrared (TIR) imagery from Landsat by prioritizing advisory texts only to over-irrigating farmers in rapidly depleting groundwater regions. The use of Landsat TIR data for tracking on-field agricultural water consumption and GRACE data for large scale groundwater depleted zone identification is now well established (this is discussed in more detail in literature review and methodology). However, to the best of our knowledge, none of the previous studies incorporated groundwater depleted zone identification from GRACE data with Landsat TIR data for an operational IAS. Resource-constrained nations in South Asia have limited capacity to maintain an irrigation advisory as a free service for all their farmers until a proper business model is developed. Thus, it is timely to investigate how the integration of satellite gravimetry with satellite TIR data can

improve the efficiency of the IAS in terms of maximizing impact for the same outreach to farmers. The key questions this study asks are as follows:

1) What is the representative scale at which GRACE TWS data should be applied for integration with an operational IAS?
2) To what extent we can independently verify GRACE-identified regions where groundwater is potentially declining due to excess irrigation during dry season?
3) What is the potential impact of irrigation water saving with an IAS enhanced with GRACE and Landsat TIR satellite data?

For answering the above-mentioned questions, we identified the groundwater depleted regions using GRACE TWS anomaly during dry season. We assessed the irrigation scenarios over those identified zones at a local/district scale. We compared the water consumed by plants over those districts with the crop water demand. To determine the actual water consumption, we computed ET using Surface Energy Balance Algorithm for Land (SEBAL) (Bastiaanssen et al., 1998a, 1998b) and the crop water demand was computed by estimating the ET based on Penman-Monteith (FAO-56) technique. Finally, from this comparison we identified the regions with excessive over-irrigation and evaluated the percent of ground water that could potentially be saved with proposed improved IAS. We also assessed the impact of existing IAS that is operationalized over some irrigation districts using SEBAL ET. Finally, we propose an enhanced IAS based on integration of GRACE gravimetry and Landsat TIR data for maximum reduction of groundwater waste for monsoon dominated regions around the world with extensive dry season irrigation practice. Figure 1.1 illustrates the steps involved in methodology.

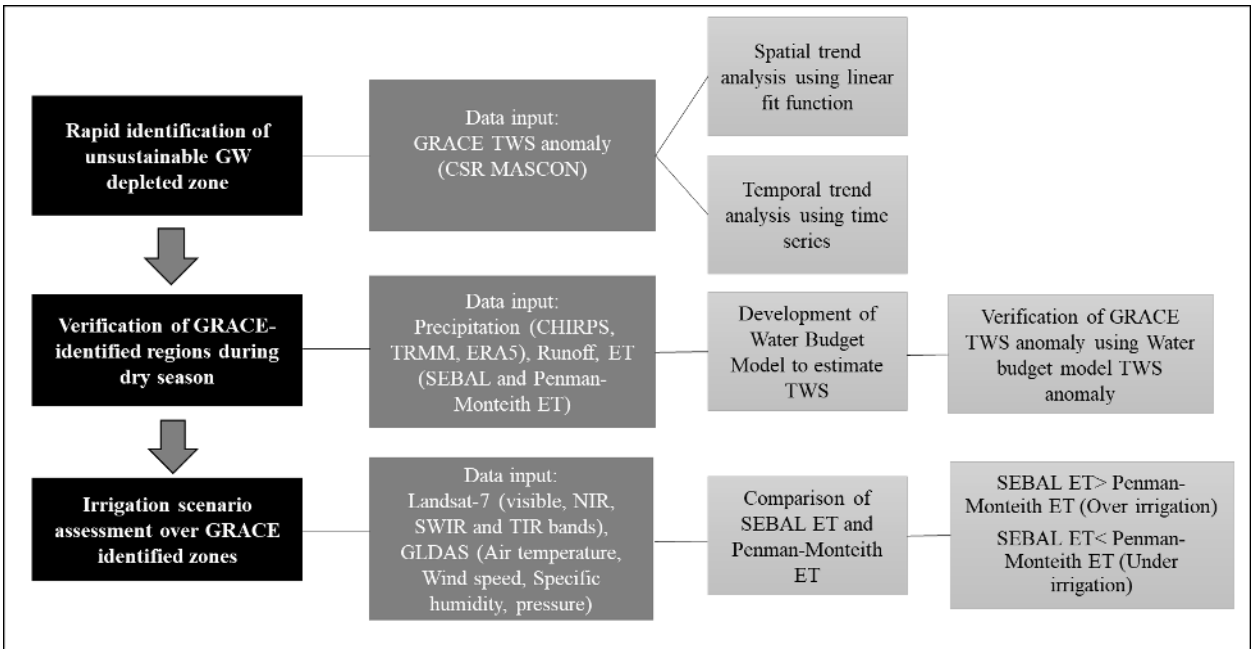

Figure 1.1. Schematic summary of steps followed in methodology.

1.4 THESIS OUTLINE

The thesis has been organized as follows. Chapter 2 gives an overview of the current scenario of groundwater resources in South Asian countries. It also outlines the relevant work done in the past or is in progress on irrigation advisory service and groundwater depleted zone identification. Chapter 3 describes the methodology that was implemented to improve the existing IAS. Essentially, it elaborates on the site selection criteria, details of associated remote sensing and in-situ data, SEBAL and Penman-Monteith ET models and steps of groundwater depleted zone identification using GRACE data. The chapter ends with the procedure of evaluating over and under-irrigation over the selected study regions. In Chapter 4, results are interpreted that are evaluated applying the steps described in Chapter 3 over the selected districts to demonstrate the effectiveness of the present study and its real-world application. Chapter 5 contains concluding remarks and directions for future study.

Chapter 2. LITERATURE REVIEW

Groundwater plays a critical role in global food security by groundwater-fed irrigation. In addition to human consumption for domestic, large volume of groundwater is required for industrial and irrigational purposes (Shah, 2007). Variability in spatiotemporal precipitation patterns and climate events makes groundwater resource dynamics sensitive to recharge. South Asia, which consumes largest volume of global groundwater resource, is facing a severe scarcity of usable waters because of population rising, urbanization, and change in water use, cropping pattern, and lifestyle. The availability of groundwater within the region is extremely variable with copious abstraction of groundwater, which is more than a quarter of the global groundwater extraction. This causes much of the region as very high water-stressed area. Hence, groundwater storage and availability in South Asia is largely based on dynamic balance between hydraulic quality of the aquifers, precipitation distribution and intensity, and human interventions by extraction or replenishment (Shah, 2007).

Many studies reported the severity of groundwater depletion in South Asia. Rodell et al. (2009) reported groundwater depletion in Rajasthan, Punjab and Haryana (figure 2.1) at a rate of 4.0 ± 1.0 cm/yr equivalent height of water, or 17.7 ± 4.5 km^3/year because of withdrawals for irrigation and other uses. They also emphasized that the difference between annual available recharge and annual withdrawals in that region was a 13.2 km^3/ year deficit according to the report of Indian Ministry of Water Resources. Figure 2.1 depicts the regions identified as critical by Indian Ministry of Water Resources. The red color denotes to the regions where groundwater withdrawals 100% exceeds recharge. However, they proved that the portion of irrigated water that replenishes the aquifers over those three districts is less and/or the rate of withdrawal is more than the Indian government estimated. Most of the groundwater withdrawn was seemed to be lost from

the region because of increases in run-off and/or evapotranspiration (irrigation). Between August 2002 and October 2008, the region lost 109 km^3 of groundwater, which is double the capacity of India's largest reservoir, the Upper Wainganga, and almost triple the capacity of the largest man-made reservoir in the United States, Lake Mead. They concluded that the depletion would likely to continue until groundwater demand is reduced or the supply or quality of the resource is diminished to the point at which farmers or locals of the areas are forced to respond. Nine years later in another study, Rodell et al. (2018) identified the rate of depletion of total water storage (TWS) to be 19.2 ± 1.1 km^3/year (half the storage capacity of Three Gorges Dam in China) in Northern India. They reported the reason to be groundwater extraction to irrigate crops, including wheat and rice, in a semi-arid climate (figure 2.2).

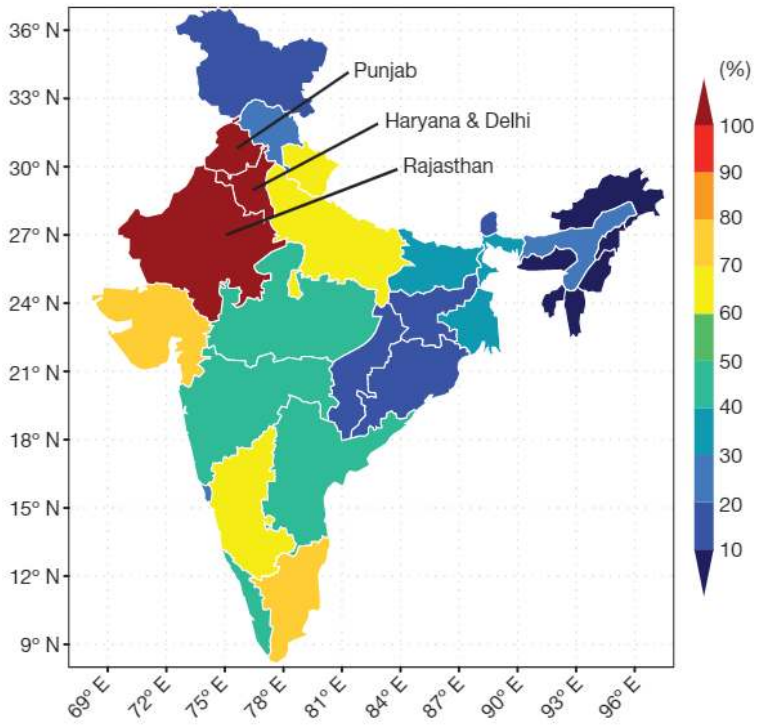

Figure 2.1. Groundwater withdrawals as a percentage of recharge. The map is based on state-level estimates of annual withdrawals and recharge reported by the Indian Ministry of Water Resources (Rodell et al., 2009; https://doi.org/10.1038/nature08238).

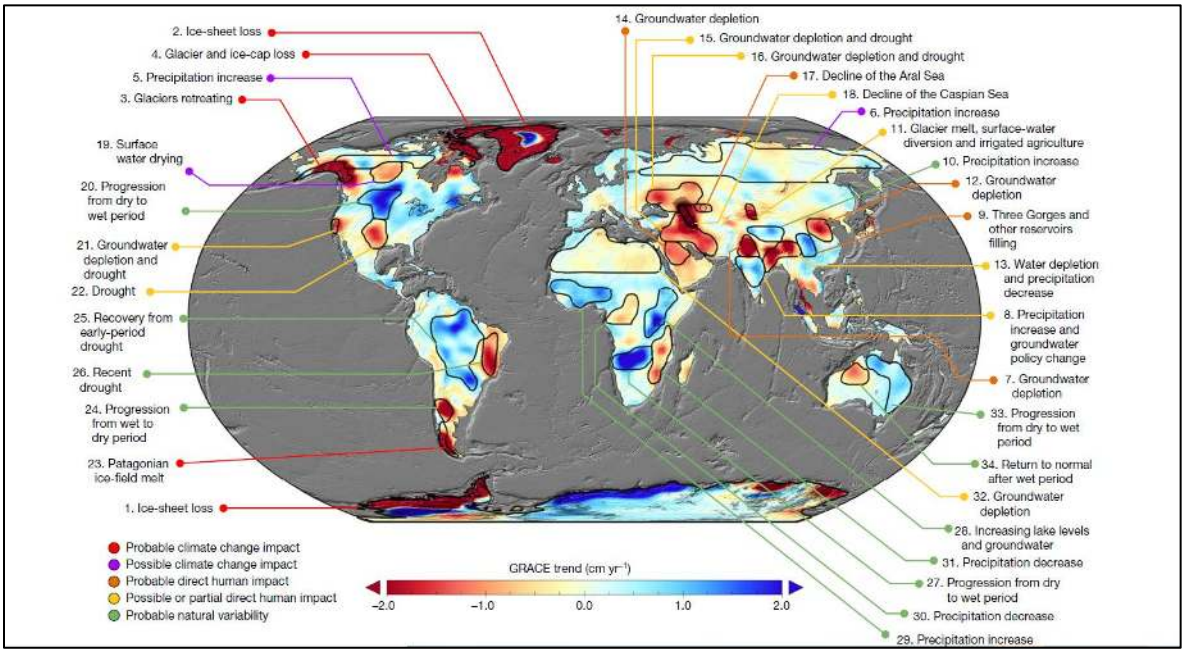

Figure 2.2. Trends in TWS (in centimeters per year) obtained based on GRACE observations from April 2002 to March 2016. The cause of the trend in each outlined study region is briefly explained and color-coded by category (Rodell et al., 2018; https://doi.org/10.1038/s41586-018-0123-1).

From 1996 to 2017 an increasing trend of groundwater storage loss has been reported over the lower Ganges basin varying from −48.83 to −2.27 cm/year during winter (or dry) seasons (November to April) (Rahman et al., 2020). That study inferred that because of groundwater irrigation and decreasing trend in rainfall during winter/dry seasons, the rate of recharge is far lower than the rate of abstraction.

Another study presented an overall trend of variations in the dynamic behavior of groundwater in Indus Basin. The reasons of groundwater depletion were attributed to the huge pumping rate for irrigation and less recharge due to little flows in two eastern rivers Sutlej and Ravi (being controlled by India) and low rainfall. According to GRACE TWS analysis this study reported that Indus basin was losing groundwater storage at a rate of 1.5 km^3/year even after accounting for monsoonal recharge (Iqbal et al., 2017, 2016). Piezometer-based investigations indicated a smaller but nevertheless non-negligible loss rate of 0.54 km^3/year (Iqbal et al., 2016). However, the overall trend remained alarmingly unsustainable irrespective of data source or method used (Iqbal et al., 2016). A recent study also reported that over exploitation of groundwater has resulted in lowering of water table in the Indus Basin with a net loss of about 1 cm/year and 118,668.16 km^3 total groundwater storage from 2010 to 2017 in the upper Indus plain (Salam et al., 2020).

All the studies above suggested how increasing groundwater-dependent irrigation is responsible for groundwater decline in IGBM basin system. In addition, as mentioned in section 1, wastage of water by irrigating excessively than the crop water demand also promotes rapid groundwater depletion. Therefore, advising farmers as per IAS could be beneficial to reduce the uncontrolled groundwater wastage and properly manage groundwater resources.

There are very few studies that initiated and evaluated the impact IAS service, especially in South Asia. A study by Ortega et al. (2005), presented the methodological aspects and results obtained from the Irrigation Advisory Service for Farmers (SIAR) of Castilla-La Mancha, Spain. Castilla-La Mancha is a semi-arid region, with a total area of 8 million ha and an irrigable area of more an 475,000 ha, where most of the irrigated areas (at least 60%) presented serious problems of water scarcity and needed improvement in the use of irrigation water. In their study, approximately 25% of the irrigated area was advised, representing about 500 collaborator farmers.

Figure 2.3 represents the steps involved in SIAR of Castilla-La Mancha and figure 2.4 represents a typical case of comparative graphics between the irrigation requirements estimated by SIAR and the effective rainfall plus irrigation supplied by the farmer. The graphs like figure 2.4 were presented to the farmers every week to assist them in irrigation decision-making. This study reported very satisfactory feedback, particularly in the areas where farmers had already participated in previous seasons. Farmers steadily increased their response to the recommendations in the new pilot areas where the SIAR was applied in the 2001–2003 campaigns.

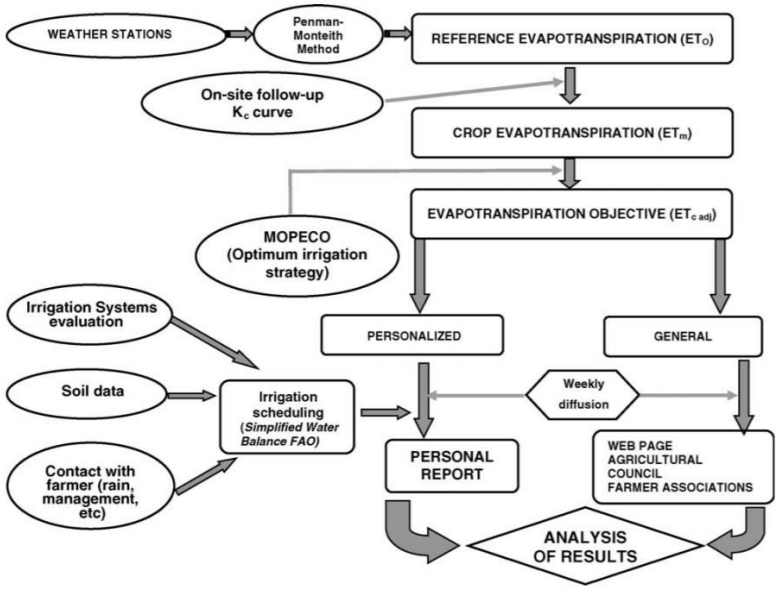

Figure 2.3. Diagram of SIAR working operation in Castilla-La Mancha (Ortega et al., 2005; https://doi.org/10.1016/j.agwat.2004.09.028).

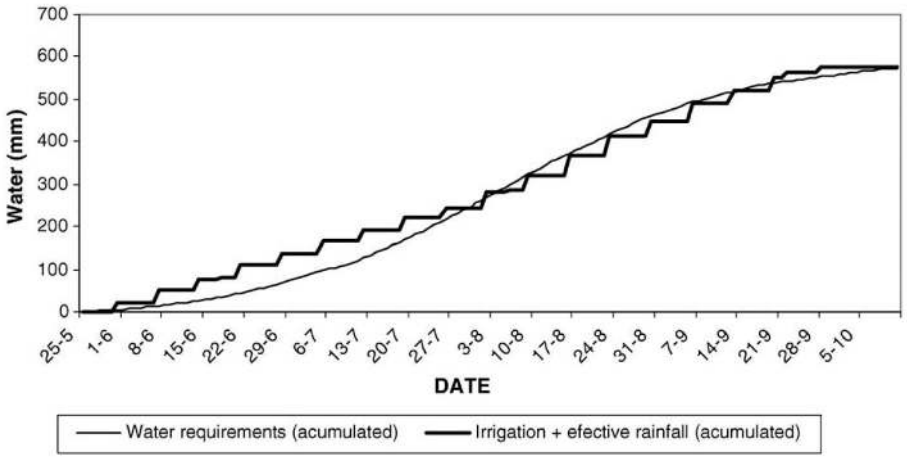

Figure 2.4. Example of comparative graphic monitoring between the irrigation requirements estimated by SIAR and effective rainfall plus irrigation supplied by the farmer, for peppers ‘‘El Picazo’’ pilot area (Ortega et al., 2005; https://doi.org/10.1016/j.agwat.2004.09.028).

Car et al. (2012) used the mobile phone Short Messaging Service (SMS) text messages as an interface to advice 72 Australian irrigators for Irrigation system dripper run time scheduling from a water balance system called IrriSat SMS. In their system, irrigators sent back information on irrigations and rainfall, also via SMS, to update the water balance. Their trial showed that a complex, water balance-based, Decision Support System (DSS) could rely on SMS as the sole interface. Figure 2.5 represents system diagram of their DSS showing components and communication methods. The engagement and utility of the system was determined by those who returned their irrigation and rainfall data; 45 sent in their data all season, 13 for half the season and 14 never sent in any data. Over all 80% of irrigators found the system useful.

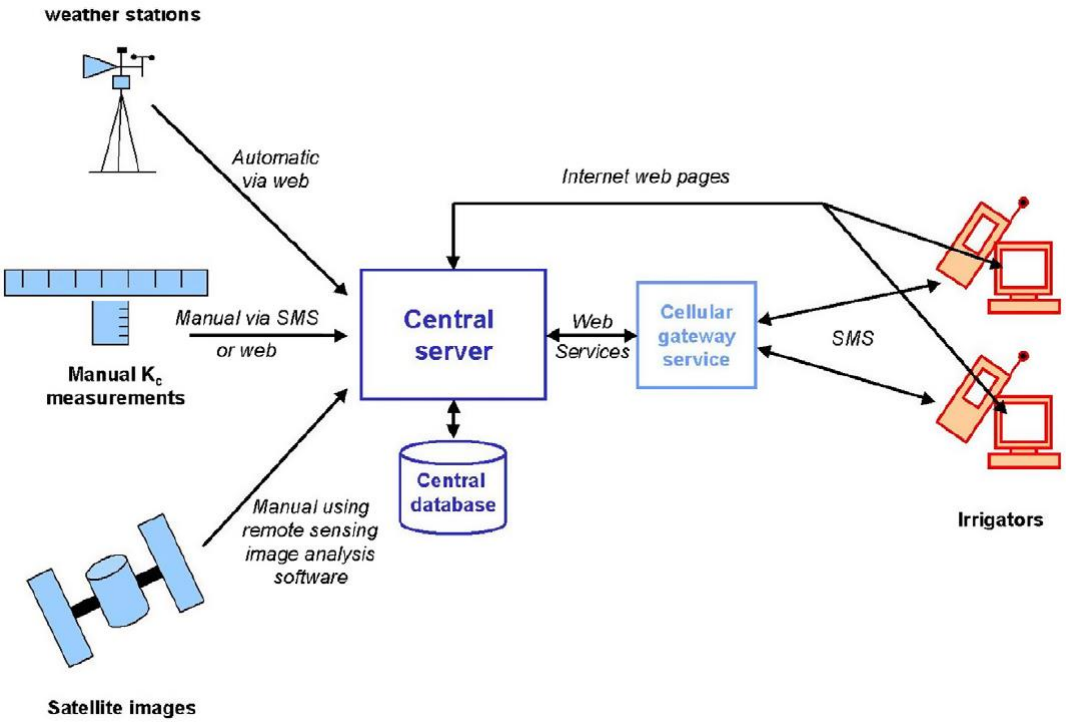

Figure 2.5. System diagram of the Decision Support System showing components and communication methods (Car et al., 2012; https://doi.org/10.1016/j.compag.2012.03.003).

In Brazil, IAS service was developed in Baixo Acaraú irrigation district, located in the north-east of Brazil. Corcoles et al. (2016) presented the results of the IAS service activities in Brazil during the 2011, 2012 and 2013 irrigation seasons. Their IAS service also calculated the emission uniformity (EU) of the system using the data collected by the technician. During the first irrigation season (2011), they observed differences between the irrigation water supplied by farmers and the irrigation water demanded by crops according to the annual relative irrigation water supply indicator. In cases of acerola, guava and gaviola, the irrigation water supply exceeded crop water requirements. During later irrigation seasons (2012 and 2013), they highlighted a good fit between irrigation water supply and crop water requirements as most of the farmers adapted IAS and followed the crop irrigation requirements advised by the IAS. At the beginning of the irrigation

season, on-field emission of uniformity was close to 67%. During the following evaluations, emission of uniformity reached 85%.

Another assessment report on water use efficiency (WUE) of IAS in Spain was published for corn yield by comparing crop coefficients from regional IAS (demand) and satellite products (consumed). It evaluated the irrigation deficit and over-irrigation based on WUE and reported deficient irrigation during dry season and full or over-irrigation during wet season over their selected irrigation districts (Segovia-Cardozo et al., 2019).

Though IAS has all the above-mentioned studies and positive impact evaluation, there is a scope of enhancement as IAS involves an operational cost. For the developing countries in South Asia minimization of operational cost with saving maximum amount of water is critical. Hence, in this study, we improved existing IAS by targeting exclusively to regions and farmers where groundwater consumption for irrigation needs to be more urgently managed for sustainability of groundwater depletion. We integrated Gravity Recovery and Climate Experiment (GRACE) TWS anomaly data with Thermal Infrared (TIR) imagery from Landsat for prioritizing advisory texts only to over-irrigating farmers. Large scale identification of groundwater depleted zones using GRACE TWS data have been reported in many studies, where they identified the regions with groundwater recharge of depletion (Bhanja et al., 2020; Castellazzi et al., 2018, 2016; Gao et al., 2020; Li et al., 2019; Richey et al., 2015; Rodell et al., 2018, 2009; Salam et al., 2020; Sarkar et al., 2020; Voss et al., 2013). However, as mentioned earlier, to the best of our knowledge, none of these studies incorporated groundwater depleted zone identification from GRACE data with Landsat TIR data for an operational IAS. Hence, with the need of improving existing IAS by prioritizing groundwater depleted and over-irrigated zones, we incorporated GRACE data and with

Landsat TIR data for maximum reduction of groundwater waste for monsoon dominated regions around the world with extensive dry season irrigation practice.

Chapter 3. METHODOLOGY

3.1 SITE SELECTION

The IGBM basin spreads across the lush plains in Pakistan, India, Bangladesh, and Nepal; one of the world's most important high yielding transboundary aquifer systems (Mukherjee et al., 2015). In this study, we considered the Ganges and Indus basins from IGBM. Rapid depletion of groundwater has been observed over Uttar Pradesh (Ganges, India) and Punjab (Indus, Pakistan). In Uttar Pradesh, the net area of irrigation dependent on groundwater is approximately 106,410 km^2 (FAO, 2016). Uttar Pradesh is divided into many irrigation districts. Based on depth to water table (DTW) analysis we selected Kanpur Nagar (3,155 km²), Kanpur Dehat (3,021 km²), Agra (4,027 km²), and Lucknow (2,530 km²) as these regions are suffering most from water scarcity during dry season (figure 3.1 a). In Kanpur Nagar, the DTW was 8 m in 2002, which has now dropped to 20 m in 2020. Similarly, in Kanpur Dehat, Agra, and Lucknow DTW dropped from 8 m to 17 m, from 15 m to 30 m and from 7 m to 20 m, respectively (WRIS India; see https://indiawris.gov.in/wris/).

In northeastern part of Punjab province in Pakistan, the declining groundwater tables are most noticed in areas with fresh groundwater (Mekonnen et al., 2016). Particularly, the Eastern Punjab is a hotspot for groundwater depletion. The net irrigation area dependent on groundwater in Punjab province is about 42,930 km^2 (FAO, 2016). For our study we selected four most vulnerable areas comprised of Sargodha (5,854 km²), Muzaffargarh (8,249 km^2), Layyah (6,291 km²), and Sheikhupra (3,030 km²) in Punjab based on DTW analysis (figure 3.1 b).

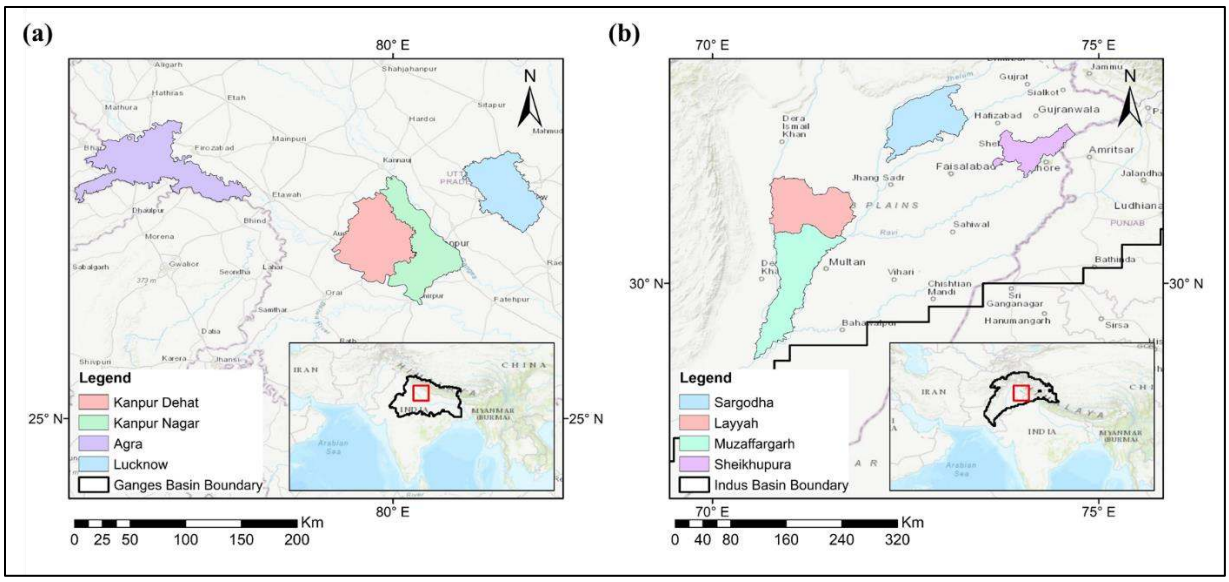

Figure 3.1. Study sites showcasing (a) four irrigation districts (Kanpur Nagar, Kanpur Dehat, Agra, and Lucknow) selected within Ganges basin and (b) four irrigation districts (Sargodha, Layyah, Muzaffargarh, and Sheikhupura) selected within Indus basin.

3.2 DATA USED

3.2.1 *GRACE TWS: Identifying Groundwater Depleted Zones*

To rapidly identify the unsustainable groundwater depleted regions (during dry season) for a more efficient IAS, GRACE TWS anomaly data for the period of 2002 to 2016 were retrieved from a cloud computing catalog (https://developers.google.com/earthengine/datasets/catalog/NASA_GRACE_MASS_GRIDS_LAND) provided by Google Earth Engine (GEE) (Gorelick et al., 2017). GRACE Tellus (GRCTellus) Monthly Mass Grids provides monthly gravitational anomalies relative to a 2004-2010 time-mean baseline. The data confined in this dataset are units of "Equivalent Water Thickness" which represent the deviations of mass in terms of vertical extent of water in

centimeters. GRACE is different from most Earth observing satellite missions because it does not measure the electromagnetic energy reflected back to it from the Earth's surface. Instead, the two GRACE satellites themselves act together as the primary instrument and orbit one behind the other in the same orbital plane at approximate distance of 220 kilometers (137 miles). As the pair orbits the Earth, areas of slightly stronger gravity (greater mass concentration) affect the lead satellite first, pulling it away from the trailing satellite. As the satellites continue along their orbital path, the trailing satellite is pulled toward the lead satellite as it passes over the gravity anomaly. Changes in the distance between these two satellites are used to make gravitational field measurements. An extremely precise microwave ranging system on GRACE detects these infinitesimal changes in the distance between the satellites. An accelerometer, located at each satellite's center of mass, measures the non-gravitational accelerations (such as those due to atmospheric drag) so that only accelerations caused by gravity are considered. Satellite Global Positioning System (GPS) receivers determine the exact position of the satellite over the Earth to within a centimeter or less. The final product which the scientists get from the GRACE satellite is spherical harmonic co-efficient, which is converted to equivalent water thickness considering the mass changes as concentrated in a very thin layer of water at the surface with changing thickness. In reality, much of the monthly change in gravity is indeed caused by changes in water storage in hydrologic reservoirs, by moving ocean, atmospheric and cryospheric masses, and by exchanges among these reservoirs. The information on detail of how GRACE satellite works can be found here: https://earthobservatory.nasa.gov/features/GRACE/page4.php. The GRCTellus dataset, which provides the equivalent water thickness, is produced by three centers: the Center for Space Research at the University of Texas at Austin (CSR MASCON), NASA Jet Propulsion Laboratory (JPL) and German Space Agency (Geoforschungszentrum, GFZ). Each center is a part of the

GRACE Ground System and generates Level-2 data (spherical harmonic fields) which are resampled to 1 degree in the GEE catalog. Here we used the CSR MASCON product with a resolution of 1 degree (~100 km).

3.2.2 *Landsat-7 Thermal IR Data: Estimation of ET*

To monitor water consumption of plants (ET), land surface temperature is an important component, which we can derive from satellite remote sensing data, specially where no ground data is available. For computing ET, we used TIR data from Landsat-7 ETM+ (Tier 1) as top of the atmosphere (TOA) radiation because TIR bands have a high spatial resolution of 60-100 m with bi-weekly temporal resolution (Senay et al., 2016). Among various ET estimation methods, in this study we used the SEBAL method for monitoring water consumption of plants (discussed later in methodology). We imported Landsat-7 ETM+ (Tier 1) TOA TIR radiation and visible/near-infrared reflectance data from GEE which were radiometrically corrected following the procedure from Chander et. al. (2009). We did not perform further ambient atmospheric corrections for the TIR radiation, as our focus was exclusively on the dry season with very low atmospheric moisture content. The Blue (0.45 - 0.52 µm), Red (0.63 - 0.69 µm), Near Infrared (0.77 - 0.90 µm), Shortwave Infrared (1.55 - 1.75 µm) bands were acquired at a resolution of 30 m and TIR band data (10.40 to 12.50 µm) was acquired at a resolution of 60 m (see https://developers.google.com/earthengine/datasets/catalog/LANDSAT_LE07_C01_T1_TOA).

3.2.3 *Meteorological Forcings*

For developing models to estimate crop water consumption and crop water demand, one of the important datasets is the meteorological forcings. In this study we used the dataset from Global Land Data Assimilation System (GLDAS) (available at:

https://developers.google.com/earthengine/datasets/catalog/NASA_GLDAS_V021_NOAH_G025_T3H). GLDAS combines satellite and ground based observed data; creates optimal fields of land surface states and fluxes. It provides 3 hourly data with a spatial resolution of 0.25 degree (~25 km). The GLDAS component inputs for both models (SEBAL and Penman-Monteith) were air temperature at 2 m, wind speed at 10 m, specific humidity, and pressure. For our purposes, using GEE, we aggregated 3 hourly data to daily data.

3.2.4 *Precipitation Products and In-situ Well Data*

For precipitation, which is a key component of water budget model, we used three different products; Climate Hazards Group InfraRed Precipitation with Station data (CHIRPS), Tropical Rainfall Measuring Mission (TRMM) and Copernicus ERA5. CHIRPS is a 35+ year quasi-global rainfall data set, spanning 50°S-50°N (and all longitudes). It provides daily data at 0.05 degree (~5 km) spatial resolution. TRMM 3B42 dataset provides a 3 hourly rainfall estimates at 0.25 degree (~25 km) resolution. ERA5 dataset provides an atmospheric reanalysis of the global climate, a fifth-generation product of European Centre for Medium-Range Weather Forecasts (ECMWF). The reanalysis integrates the model data with complete and consistent observations from across the world into a global dataset. The daily total precipitation values in ERA5 are given as daily sums with a spatial resolution 0.25 degree (~25 km). For our purposes, we aggregated all three precipitation datasets to monthly accumulations. All three of these datasets can be accessed from the GEE catalog at https://developers.google.com/earth-engine/datasets/catalog.

To understand if on-farm water consumption according to SEBAL ET during dry season is a proxy for groundwater withdrawals, we used in-situ DTW data. For irrigation districts within Ganges basin, we used a data portal named Water Resources Information System of India (WRIS India; see https://indiawris.gov.in/wris/). Figure 3.2 portrays the interface of WRIS, India. For

irrigation districts within Indus basin we used sampled piezometer data provided by PCRWR (Iqbal et al., 2017).

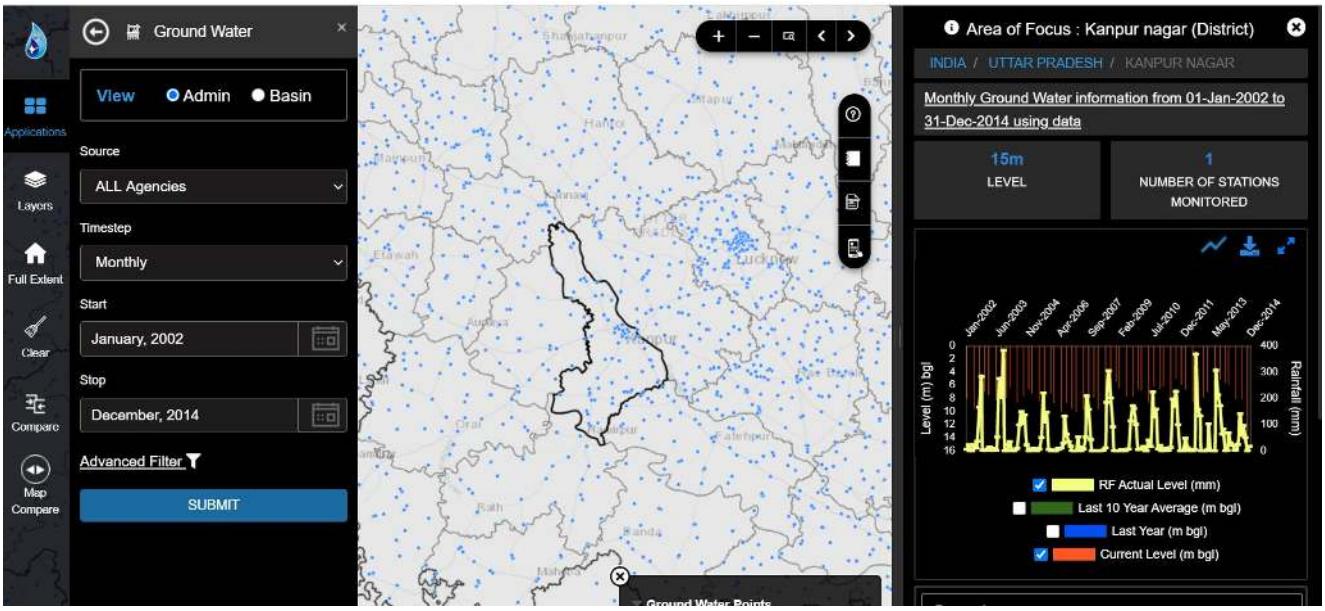

Figure 3.2. Interface of data portal Water Resources Information System of India (WRIS India; see https://indiawris.gov.in/wris/).

3.3 SEBAL Evapotranspiration

For quantifying actual water consumption (ET) variability where availability of ground-based data is a constraint, various satellite-based methods are reported in literature. SEBAL and METRIC (Mapping Evapotranspiration at High Resolution and with Internalized Calibration) are such two widely-used techniques (Liou and Kar, 2014). In our study we implemented SEBAL which has already been effectively implemented in many studies to assess actual ET using satellite images (Ghaderi et al., 2020; Senay et al., 2016). The steps followed in this study for SEBAL ET calculation is presented in advanced training and user's manual of SEBAL by Waters et al., 2002. This manual is available freely as pdf version, see here: http://www.posmet.ufv.br/wp-

content/uploads/2016/09/MET-479-Waters-et-al-SEBAL.pdf. SEBAL model solves the surface energy balance to compute ET using satellite images and weather data. Since the satellite image provides information for the overpass time only, SEBAL computes an instantaneous ET flux for the image time. A series of equations are incorporated in SEBAL model that compute net surface radiation, soil heat flux, and sensible heat flux to the air (figure 3.3). The residual energy flux is then calculated by subtracting the soil and sensible heat fluxes from the net radiation at the surface. This residual energy (latent heat) enables liquid water to phase transition to water vapor, *i.e.*, evapotranspiration. Thus, for each pixel of the image, the ET flux is calculated as a residual of the surface energy budget equation:

$$\lambda ET = Rn - G - H \quad (3.1)$$

Where, λET is the latent heat flux (W/m^2), Rn is the net radiation flux at the surface (W/m^2), G is the soil heat flux (W/m^2), and H is the sensible heat flux (W/m^2).

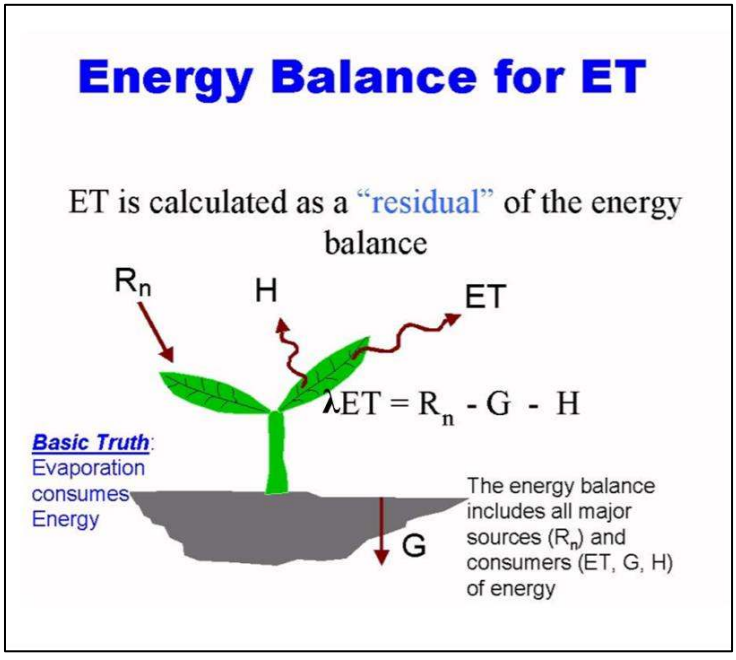

Figure 3.3. SEBAL ET estimation using Surface Energy Balance algorithm (Waters et al., 2002).

The first step in the SEBAL procedure is to compute the net surface radiation flux (Rn) using the surface radiation balance equation:

$$Rn = (1 - \alpha)\, RS\downarrow + RL\downarrow - RL\uparrow - (1 - \varepsilon o)RL\downarrow \quad (3.2)$$

Where, RS↓ is the incoming shortwave radiation (W/m^2), α is the surface albedo (dimensionless), RL↓ is the incoming longwave radiation (W/m^2), RL↑ is the outgoing longwave radiation (W/m^2), and εo is the surface thermal emissivity (dimensionless) (figure 3.4). Figure 3.5 presents the steps involved in net radiation calculation.

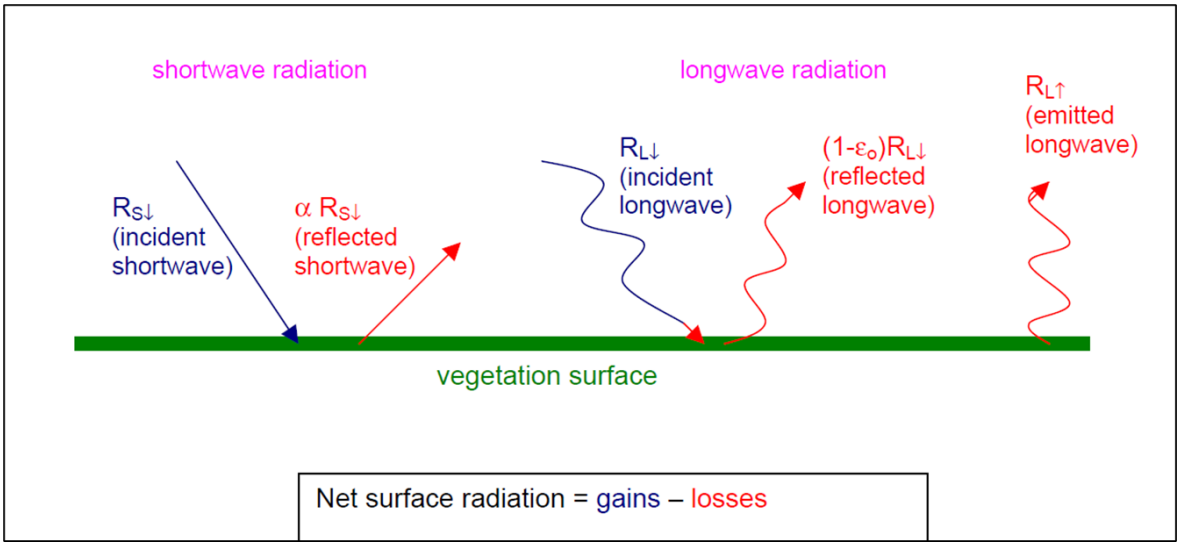

Figure 3.4. Surface radiation balance for net radiation estimation (Waters et al., 2002).

Next, soil heat flux, the rate of heat storage into the soil and vegetation due to conduction, was calculated by first computing the ratio G/Rn using the following empirical equation (Waters et al., 2002):

$$G/Rn = Ts/\alpha\,(0.0038\alpha + 0.0074\alpha^2)(1 - 0.98NDVI^4) \quad (3.3)$$

Where, Ts is the surface temperature (Celsius), α is the surface albedo, and NDVI is the Normalized Difference Vegetation Index. G is then readily calculated by multiplying G/Rn by the value for Rn computed previously.

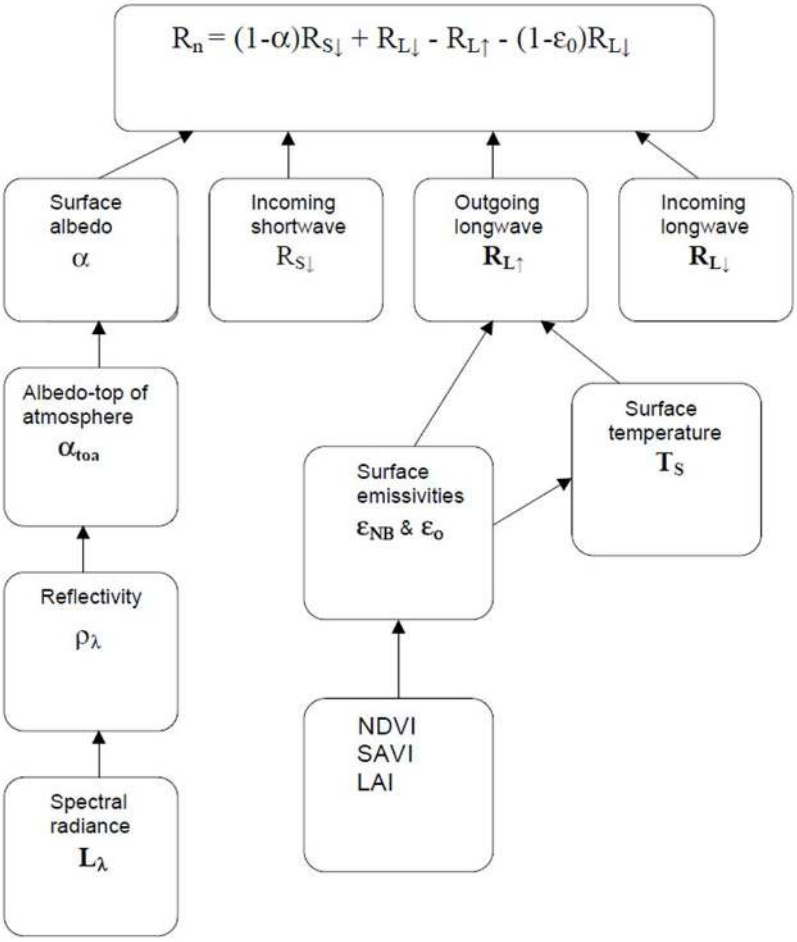

Figure 3.5. Steps and parameters involved in net radiation estimation (Waters et al., 2002).

Finally, Sensible heat flux, the rate of heat loss to the air by convection and conduction, due to a temperature difference, was computed using the following equation for heat transport (Waters et al., 2002):

$$H = (\rho \times cp \times dT) / rah \quad (3.4)$$

Where, ρ is air density (kg/m^3), cp is air specific heat (1004 J/kg/K), dT (K) is the temperature difference ($T_1 - T_2$) between two heights (z_1 and z_2), and rah is the aerodynamic resistance to heat transport (s/m).

3.4 PENMAN-MONTEITH EVAPOTRANSPIRATION

Penman-Monteith ETo, which is a proxy to potential water demand for reference crop, was calculated over the selected districts following the steps from Allen et al., (1998). The equation for ETo is as follows:

$$ET_o = \frac{0.408\,\Delta\,(R_n - G) + \gamma \frac{900}{T+273}\,u_2\,(e_s - e_a)}{\Delta + \gamma\,(1 + 0.34\,u_2)} \quad (3.5)$$

where, ET_o is reference evapotranspiration (mm/day), R_n is net radiation (MJ m^{-2} day^{-1}), G is ground heat flux (MJ m^{-2} day^{-1}), considered negligible (i.e., 0) here, T is mean air temperature at 2 m height (˚C), u_2 is wind speed at 2 m height (m/s), e_s saturation vapor pressure (kPa), e_a actual vapor pressure (kPa), Δ is slope of saturation vapor pressure (kPa ˚C^{-1}), γ is psychrometric constant (kPa ˚C^{-1}).

ETo calculated using equation 3.5 is for a reference crop (grass of 0.12 m height) which is then converted for the actual crop growing in the selected districts. For this we considered the crop type, development stage, and the relative soil saturation (or stress). As wheat was the dominant crop in our study regions, we used the corresponding crop coefficient (Kc) referred in FAO, 2020 and assumed soil water stress coefficient (Ks) of 0.5, which in our experience is representative of stress conditions during the dry season. We multiplied Kc and Ks with ETo to derive the crop water demand for wheat over the study regions, which is illustrated in figure 3.6.

After calculation of SEBAL and Penman-Monteith ET, a scenario of over-irrigation was identified when actual water consumption (SEBAL ET) was found to be greater than the crop

water demand (Penman-Monteith ET). Similarly, when actual water consumption was found to be less than the crop water demand, the scenario was flagged as under-irrigation. Finally, the percent of over or under irrigation over those regions and how much irrigated water can be potentially saved was evaluated with improved IAS during dry season (detail in section 3.7).

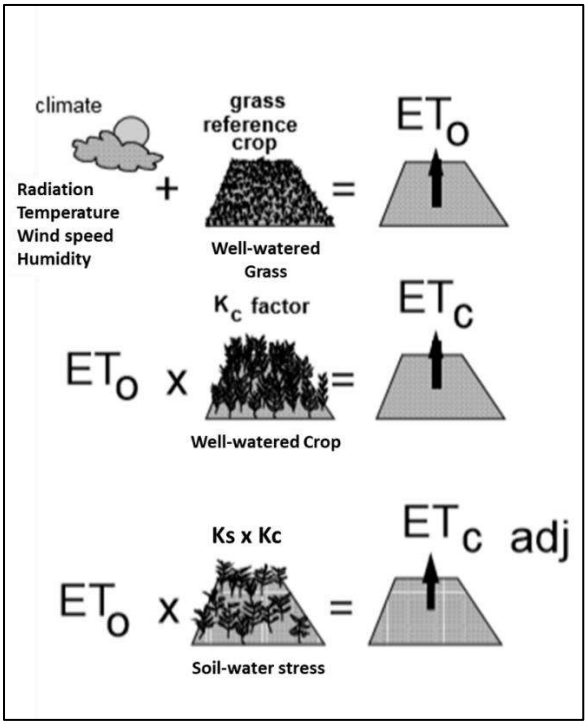

Figure 3.6. Conversion of Penman-Monteith reference ET to actual ET (FAO 2016).

3.5 Spatial and Temporal Trend of GRACE TWS Anomaly

To understand the trends in groundwater storage from 2002 to 2016, we fit a linear model. Considering January to December for CSR MASCON product of GRACE TWS anomaly over the entire time period, we developed a linear regression model. Here, we assumed that GRACE TWS

anomaly is a strong proxy for groundwater storage change during dry season in monsoon climates based on the water budget equation as follows:

$$\Delta S = P - Q - ET \quad (3.6)$$

In above equation 3.6, ΔS, P, Q and ET are total/terrestrial water storage change, precipitation, surface run-off and evapotranspiration, respectively. The total storage change can be further broken down into the following four components.

$$\Delta S = \Delta GWS + \Delta SM + \Delta SWE + \Delta SW \quad (3.7)$$

Here, ΔGWS, ΔSM, ΔSWE, and ΔSW are storage change components for GW, soil moisture, snow water equivalent, and surface water, respectively.

During dry season in South Asian countries, there is negligible precipitation or surface run-off. Hence, P and Q are near-zero and thus, ΔSM and ΔSW are also negligible. Given no snow-covered areas in the Gangetic and Indus plains of South Asian countries, ΔSWE is also equivalent to zero. Therefore, we are left with the simplified form for equation 3.7 for South Asia during dry season, i.e., ΔS = ΔGWS. This is the basis of our hypothesis for using GRACE TWS anomaly as a proxy for groundwater storage change during dry season, which we later demonstrate as having a sound basis.

3.6 Representative GRACE Data Scale for Identifying Groundwater Depleted Zones

For identifying the representative scale at which GRACE can be used to rapidly identify the fast depleting zones, we compared GRACE TWS anomaly against the water budget model derived TWS anomaly. First, we divided the entire Ganges basin into 5 sub-basins based on the stream orders as shown in figure 3.7. We defined the stream order based on Strahler's classification

(Fitzpatrick et al. 1998). The higher ordered sub-basins included all the lower order sub-basins. After sub-basin delineation, we developed the water budget model from 2002-2014 using equation 3.6 and implemented over each sub-basin followed by estimating TWS. For model inputs, three different precipitation products (CHIRPS, TRMM and ERA5) were used to address the uncertainty embedded with satellite products, run-off from Variable Infiltration Capacity (VIC) (Siddique-E-Akbor et al., 2014; Wood and Lettenmaier, 1996) model, and ET from SEBAL model (equation 3.1).

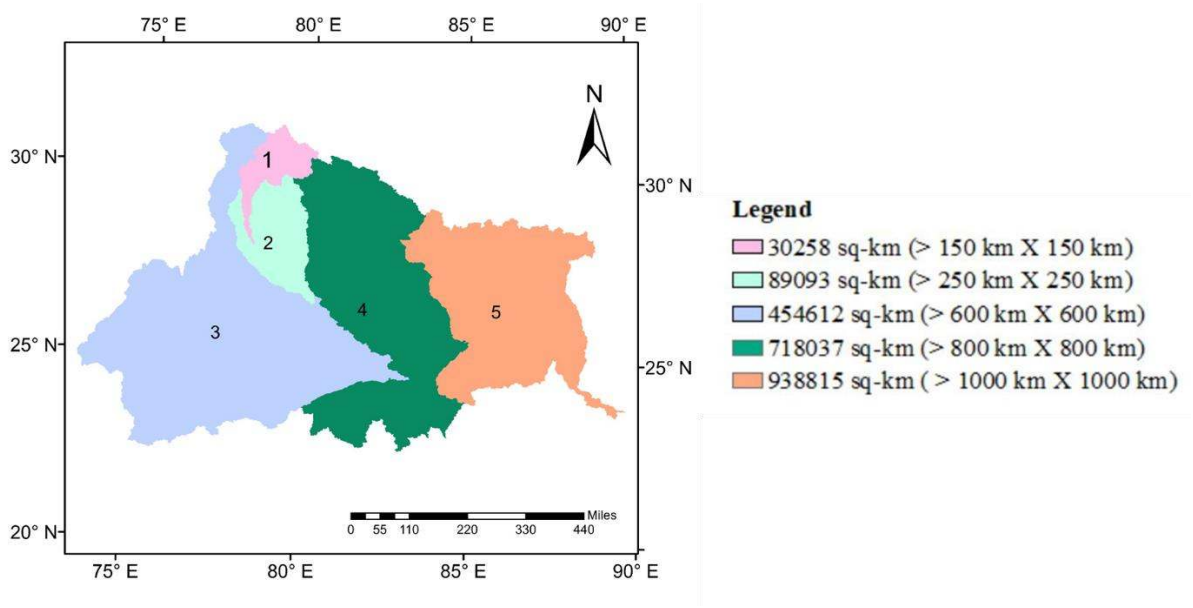

Figure 3.7. Delineation of sub-basins based on stream orders for water budget model development over Ganges basin. On the right, different colors incorporate to corresponding areas and respective scales of each sub-basin.

For the ET component of the water budget model (equation 3.6), we applied SEBAL using Landsat-7 satellite images. The SEBAL model also required the meteorological data including wind speed, surface pressure, specific humidity, and air temperature as inputs for solving the surface energy balance calculation (equation 3.1). We used GLDAS outputs as meteorological forcing input for the SEBAL model. To avoid the non-cropped areas, we used the crop map from

Global Food Security Support Analysis Data (GFSAD) Crop Dominance Global 1 kilometer (km) (can be accessed here: https://lpdaac.usgs.gov/products/gfsad1kcmv001/).

It is worth mentioning that there are alternate approaches for satellite-based ET estimation. For example, the VI-Ts method has been used to compute actual ET or crop water consumption (Tang et al., 2009). The spatial and temporal resolutions (250 to 1,000 m and 3 to 7 days, respectively) in that study were afforded by Moderate Resolution Imaging Spectroradiometer (MODIS). MODIS is a key instrument aboard the Terra (originally known as EOS AM-1) and Aqua (originally known as EOS PM-1) satellites (see: https://modis.gsfc.nasa.gov/about/). Tang et al. (2009) used different MODIS parameters to compute the crop water consumption and verified the results by modifying METRIC algorithm based on SEBAL (Tang et al., 2009). In our study, we used Landsat images (temporal frequency 16 days) which are not as frequent as MODIS. However, for the objective of our study, the spatial resolution (from Landsat) is more important than temporal frequency in general because farmers do not need to make irrigation decisions about their crops every day or week, especially for wheat.

Next, water budget derived TWS and GRACE TWS datasets were compared over each individual sub-basin. The desired scale was selected after analyzing the bias, root mean square error (RMSE), and Spearman's rank coefficient between water budget derived TWS and GRACE TWS anomaly.

3.7 Irrigation Scenario Assessment

We quantified actual (on-farm) irrigation scenario over the selected regions to find if over-irrigation was triggering groundwater depletion. First, we performed supervised classification technique (random forest classification scheme) to differentiate cropped and uncropped regions

within the selected irrigation districts. We used Landsat-7 images and trained the classification model using four land covers; crop, forest, water, and urban to derive the land use with crops only (the latter three were grouped as uncropped) as shown in figures 3.8 and 3.9. Wheat being the dominant crop from November to April (FAO, 2020) in the selected districts, we considered wheat growing over the entire cropped regions and proceeded with further analysis.

Next, we applied SEBAL and Penman-Monteith methods on the cropped regions from 2002 to 2014 to obtain the actual water consumed by plants and water required, respectively. Finally, we used equation 3.8 to obtain the percentage of over or under irrigation happening over the selected districts comparing two sets of ETs.

Percent of over/under irrigation =

$$\frac{Actual\ water\ consumed\ (SEBAL\ ET) - Water\ Needed(Penman-Monteith\ ET)}{Water\ Needed\ (Penman-Monteith\ ET)} x100 \qquad (3.8)$$

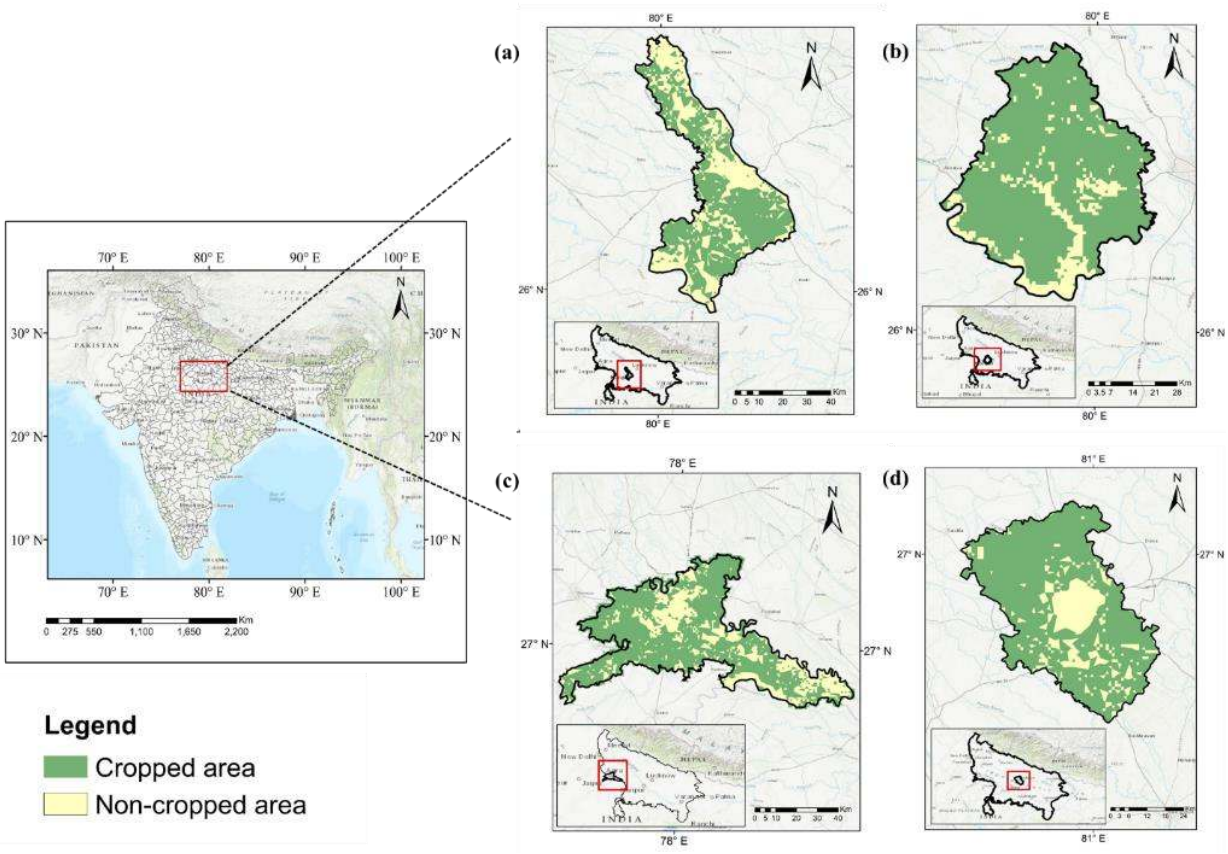

Figure 3.8. Crop maps over (a) Kanpur Nagar, (b) Kanpur Dehat, (c) Agra, and (d) Lucknow. Here, Green legend corresponds to the cropped areas.

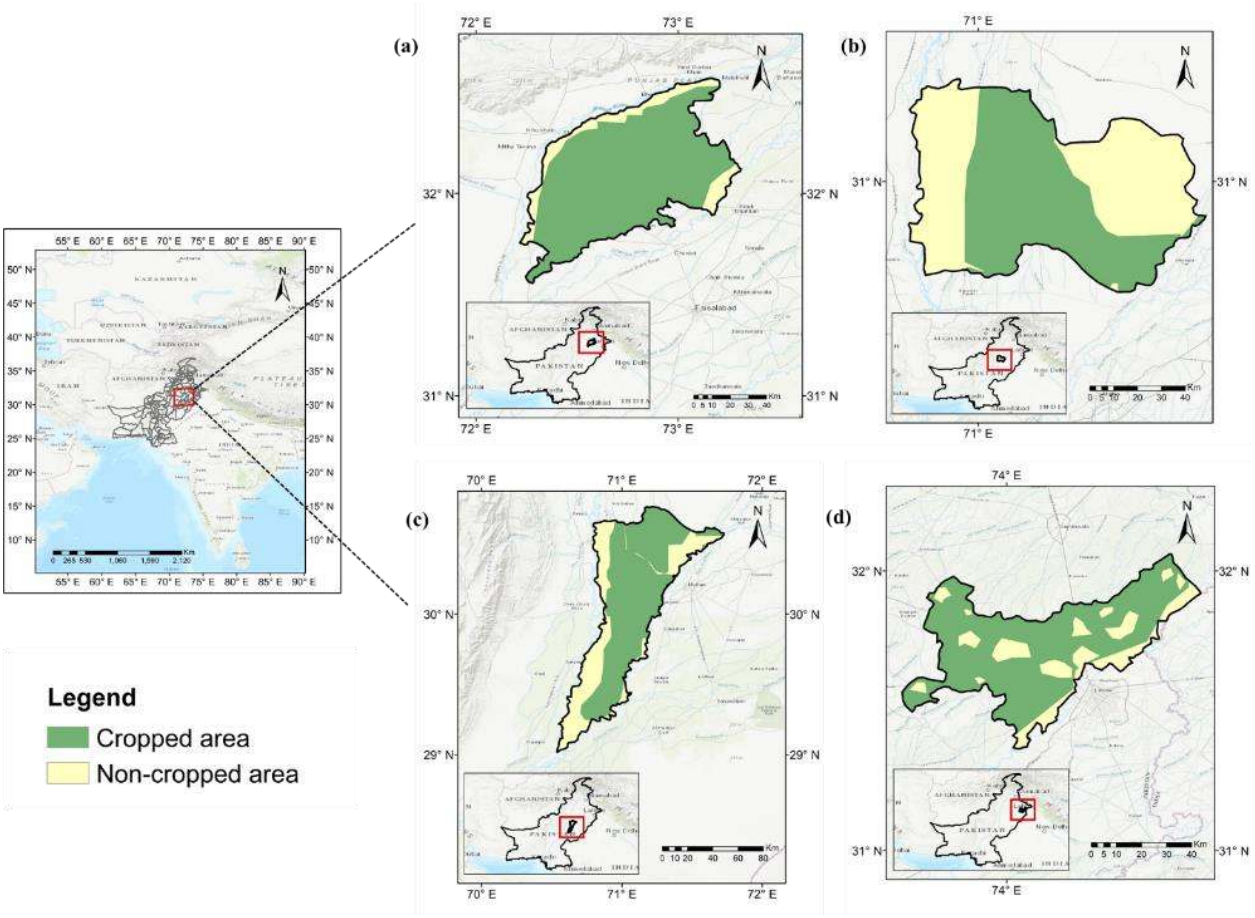

Figure 3.9. Crop maps over (a) Sargodha, (b) Layyah, (c) Muzaffargarh, and (d) Sheikhupura. Here, Green legend corresponds to the cropped areas.

Chapter 4. RESULTS AND DISCUSSIONS

4.1 Spatial and Temporal Trend of GRACE TWS Anomaly

Understanding the spatial and temporal trends of groundwater depletion is key to finding the vulnerable zones for precision targeting for an improved IAS. The spatial trend of groundwater depletion observed using regression model over Ganges basin from 2002 to 2016 is depicted in figure 4.1 (a). The GRACE TWS anomaly, already noted as a proxy for groundwater change during dry season, showed a maximum negative trend of 1.99 cm/year equivalent height of water. This means the maximum rate of groundwater depletion over the Ganges basin is 1.99 cm/year. The most alarming finding is the overall descending trend suggesting a continuous depletion over the basin regardless of wet or dry seasons. That indicates, even with the wet season recharge phase, overall (net) groundwater storage continues to decline. We studied the temporal trend of averaged TWS anomaly over the basin and observed a declining trend of 1.2 cm/year (figure 4.1 b). Though we found a maximum positive trend/groundwater recharge of 0.52 cm/year over the lower part of the basin, the overall temporal trend suggested a depletion for the entire basin (figure 4.1).

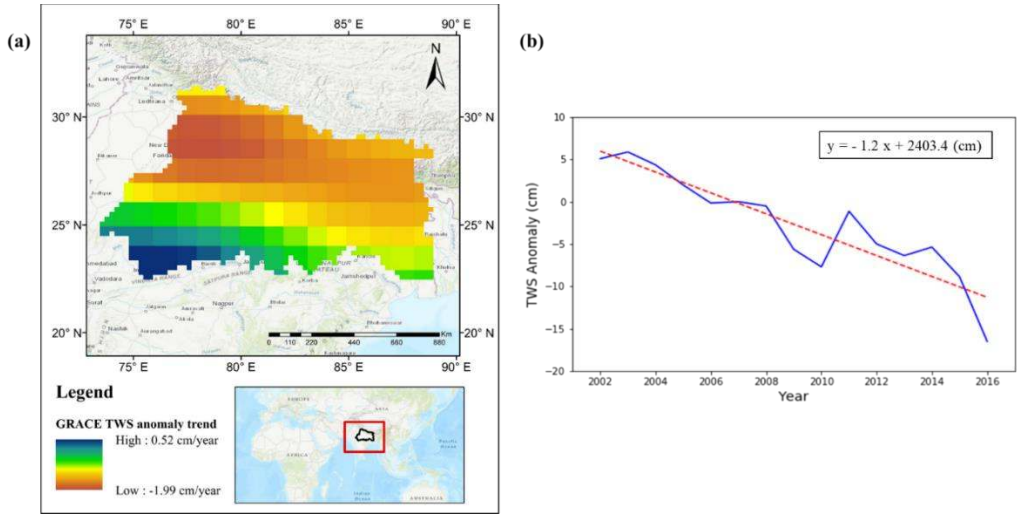

Figure 4.1. (a) Spatial and (b) temporal trend of GRACE TWS anomaly over Ganges basin from 2002 to 2016. The dark orange color in (a) represents the maximum negative rate of TWS anomaly (-1.99 cm/year) and the dark blue color represents the maximum positive rate of TWS anomaly (0.52 cm/year).

4.2 Identifying GRACE Spatial Scale of Analysis

Since we observed a negative trend of groundwater storage change over the Ganges basin (~80% area), we needed to find the scale at which GRACE can be incorporated with IAS to prioritize the zones for the improved IAS. We identified the representative scale by comparing GRACE TWS anomaly against the water budget model derived TWS anomaly derived from independent datasets. To compare these two sets of data, we used bias, RMSE, and Spearman's ranked coefficient as described in methodology. Our results suggested that from sub-basin 3 (scale 600 km X 600 km), GRACE TWS anomaly matches closely with TWS anomaly from an independent water budget model (figure 4.2). For example, the bias (figure 4.2 a) between the two TWS for sub-basins 1 and 2 varies from 19% to 26% and 17% to 23%, respectively (considering different precipitation products). However, the bias varies from 3% to 7% only when we considered sub-basin 3.

Similarly, the spearman's ranked coefficient (figure 4.2 b) for sub-basins 1 and 2 varies from -0.36 to 0.05 and -0.35 to 0.05 respectively, whereas for sub-basin 3 the coefficient varies from 0.51 to 0.54. The RMSE (figure 4.2 c) over sub-basins 1 and 2 varies from 12.7 cm to 14.7 cm (~ 58 km^3 to 67 km^3) and 12.5 cm to 14.5 cm (~ 57 km^3 to 66 km^3) respectively, whereas over sub-basin 3 it varies from 10.2 cm to 11.1 cm (~ 46 to 50 km^3). As all the indices started to show better relationship between GRACE TWS and Water budget derived TWS on sub-basin 3, we decided to select the corresponding scale of 600 km X 600 km as the optimum scale to integrate GRACE TWS data with Landsat TIR data.

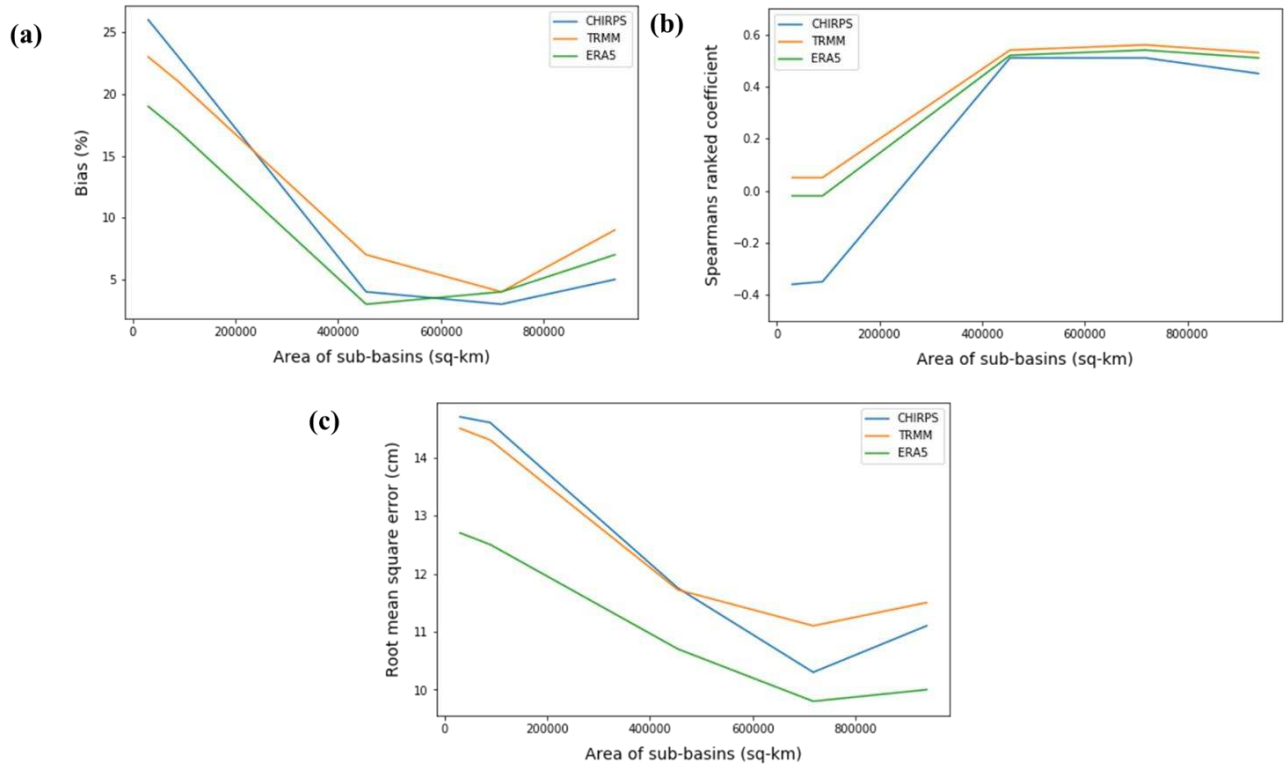

Figure 4.2. (a) Bias, (b) Spearman's rank coefficient, and (c) RMSE between GRACE TWS and water budget TWS anomalies from 2002 to 2014. Different colors represent results for different precipitation products (blue: CHIRPS, orange: TRMM and green: ERA5).

4.3 GRACE TWS VALIDATION USING WATER BUDGET APPROACH

We further verified GRACE-identified regions where groundwater is potentially declining due to excessive dry season irrigation at the selected scale of 600 km X 600 km (sub-basin 3 of Ganges basin). We compared the dry (winter) season averaged GRACE TWS and water budget TWS anomalies from 2002 to 2014. The results showed a similar decreasing pattern of GRACE TWS and water budget derived TWS anomalies, particularly from 2005 onwards (figure 4.3). This similarity in trends between TWS derived from two sets of independent datasets support our hypothesis that GRACE TWS is a strong proxy for groundwater storage change during the dry season. The delta between two sets of TWS anomalies is expected considering the uncertainties involved in the water budget model. The blue curve in figure 4.3 represents the water budget TWS anomaly using SEBAL ET. It essentially represents the actual ground condition of what was happening from 2002 to 2014. As SEBAL ET is the actual water consumption by plants, the storage change observed using SEBAL ET is a representation of actual storage change over the irrigated lands. As the decreasing storage pattern is clearly related to increasing SEBAL ET during dry season, we can postulate that the total storage or groundwater storage is going down due to increasing groundwater irrigation. A similar decreasing pattern indicates that dry season GRACE TWS can capture the signal of groundwater storage decline due to excessive dry season irrigation.

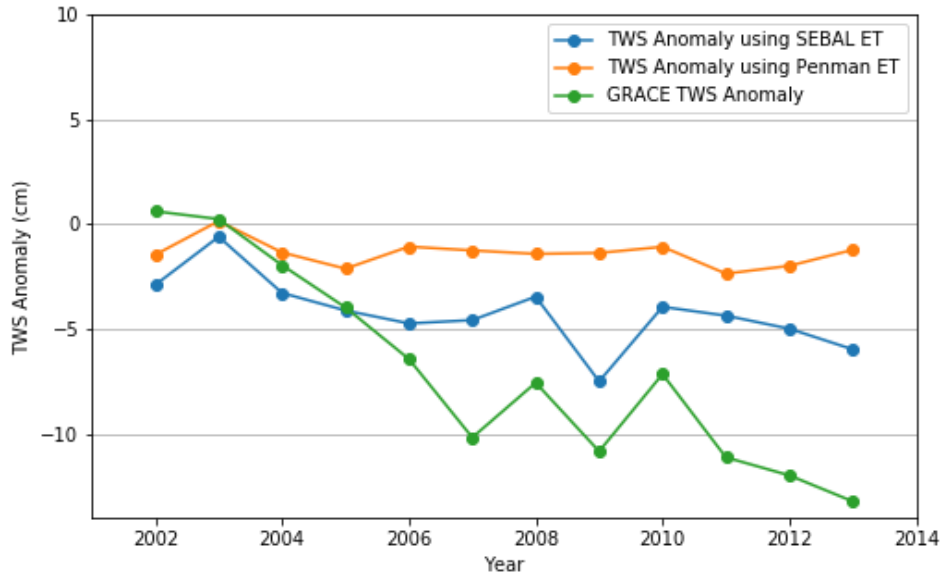

Figure 4.3. Verification of GRACE-identified region over sub-basin 3 of Ganges basin (figure 3.7) where groundwater is potentially declining due to excessive dry season irrigation using water budget derived TWS. Green line represents dry season GRACE TWS, blue line represents dry season water budget derived TWS using SEBAL ET, and orange line represents water budget derived TWS using Penman-Monteith ET.

The orange curve in figure 4.3 shows another set of water budget derived TWS obtained using Penman-Monteith ET instead of SEBAL ET. As discussed before, the Penman-Monteith ET is the crop water demand, hence the TWS we are getting using Penman-Monteith ET is representing the scenario if need based irrigation (i.e. irrigating according to crop water demand) had been undertaken hypothetically from 2002-2014. We observed that switching to need based irrigation over the selected scale can potentially arrest the current depletion trends of groundwater (net change becomes negligible; figure 4.3). We found that there is no declining trend of TWS when Penman-Monteith ET (need-based irrigation) is used in lieu of actual (SEBAL) ET that represents today's rampant waste of groundwater. Thus, we can postulate that it is theoretically possible to

save extensive amounts of irrigation water during dry season by prioritizing the critical zones based on an IAS that can facilitate crop water need-based irrigation.

4.4 VERIFICATION OF SEBAL ET OVER CROPPED REGIONS

Our proposed integration of GRACE TWS and LANDSAT TIR data in an operational IAS is valid when we compare the relationship between SEBAL ET and groundwater table data. Before quantifying the impact of improved IAS, we verified the actual water consumption (ET) according to SEBAL method using DTW data to prove that the actual water consumption (SEBAL ET) is a proxy to groundwater table decline over dry season irrigated regions.

The correlation coefficients of dry season accumulated SEBAL ET and dry season average DTW over the cropped regions of Kanpur Nagar, Kanpur Dehat, Agra, and Lucknow of Northern India are 0.76, 0.71, 0.79 and 0.75, respectively (figure 4.4). Similarly, the correlation coefficients over the cropped regions of Sargodha, Layyah, Muzaffargarh, and Sheikhupura in Eastern Pakistan are 0.87, 0.79, 0.75 and 0.85, respectively (figure 4.5). These positive correlations indicate that with increasing ET (crop water consumption), the DTW increases consistently (water table lowers). Such consistent correlation provides strong evidence that actual water consumption (SEBAL ET) is a strong proxy for groundwater table decline during dry season over irrigated landscapes of South Asia.

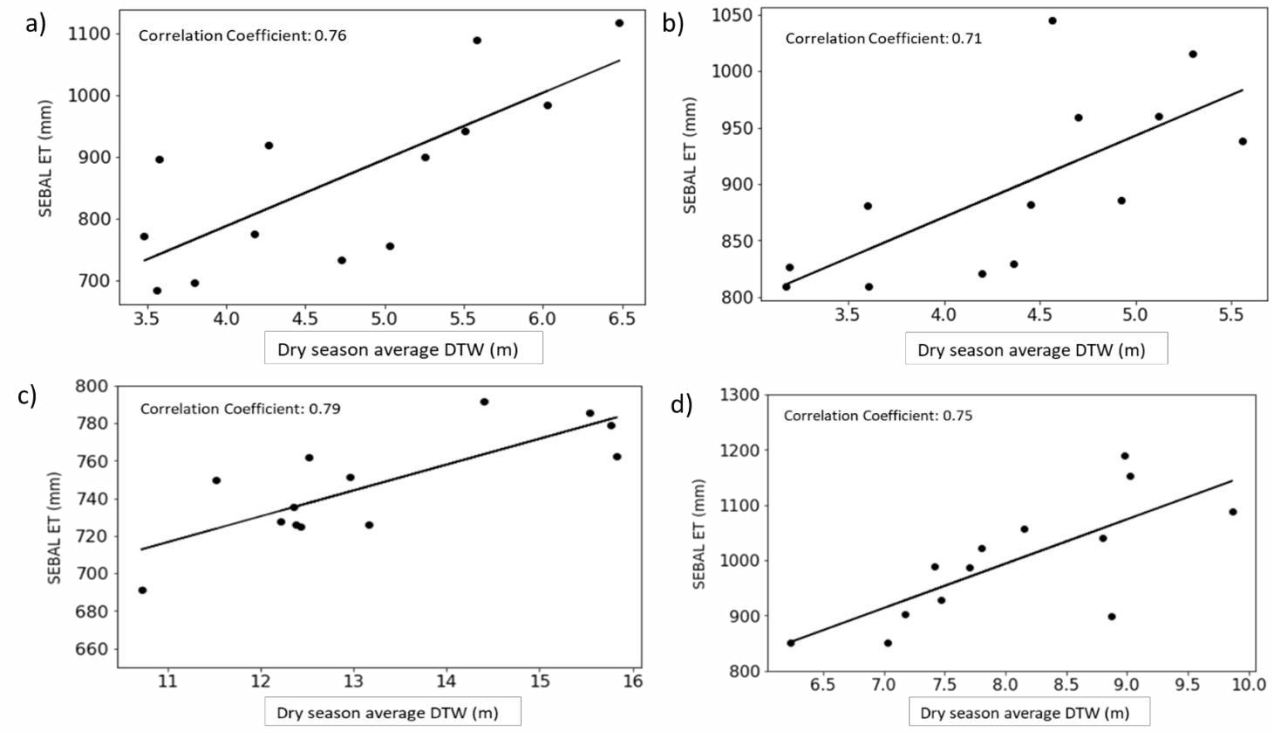

Figure 4.4. Correlation between SEBAL ET and depth to water table (DTW) during dry season (2002 to 2014) over cropped regions of (a) Kanpur Nagar, (b) Kanpur Dehat, (c) Agra, and (d) Lucknow. Each circle represents a dry season.

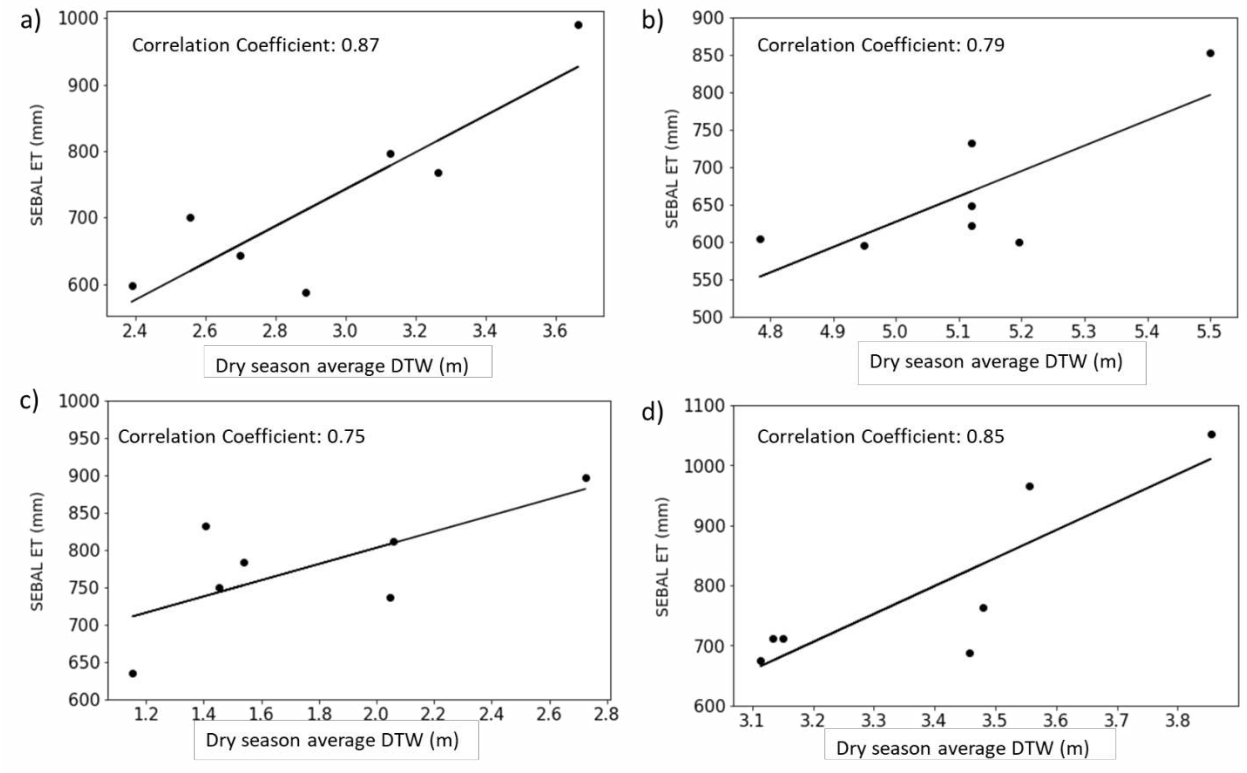

Figure 4.5. Correlation between SEBAL ET and depth to water table (DTW) during dry season (2005 to 2013) over cropped regions of (a) Sargodha, (b) Layyah, (c) Muzaffargarh, and (d) Sheikhupura. Each circle represents a dry season.

To further prove the role of SEBAL ET as a proxy for groundwater table change, we compared the DTW data over non-cropped regions (i.e. "control" or "placebo" regions where no crops are grown) of selected districts (Kanpur Nagar, Agra, and Lucknow) with SEBAL ET. We reported a low negative and near-zero correlation (figures 4.6 to 4.8). For Kanpur Nagar, Agra, and Lucknow, the correlation coefficients of SEBAL ET and DTW are -0.17, -0.31, -0.03, respectively over non-cropped regions (figures 4.6 to 4.8). These correlations indicate that with increasing DTW (decreasing groundwater table), actual ET is not increasing over non-cropped (i.e., non-irrigated) regions. As the control points are over urbanized areas, we can speculate that the groundwater table is getting extracted to lesser amounts for non-agricultural purposes.

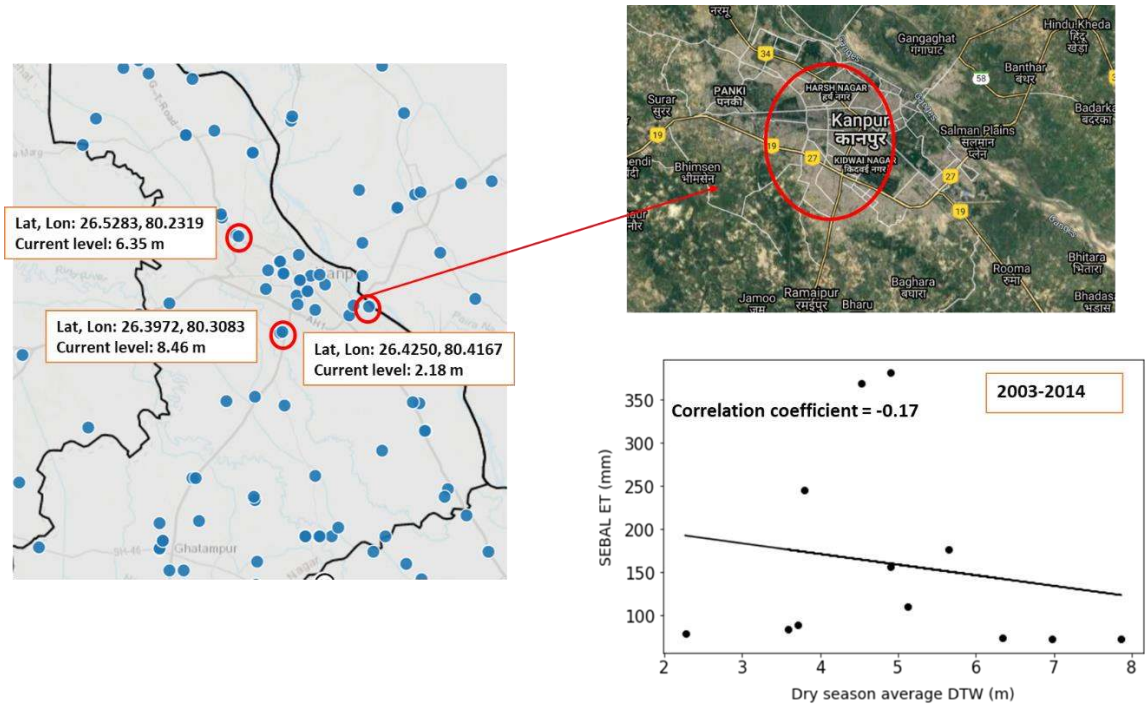

Figure 4.6. Correlation between SEBAL ET and DTW during dry season over control regions (non-cropped) of Kanpur Nagar.

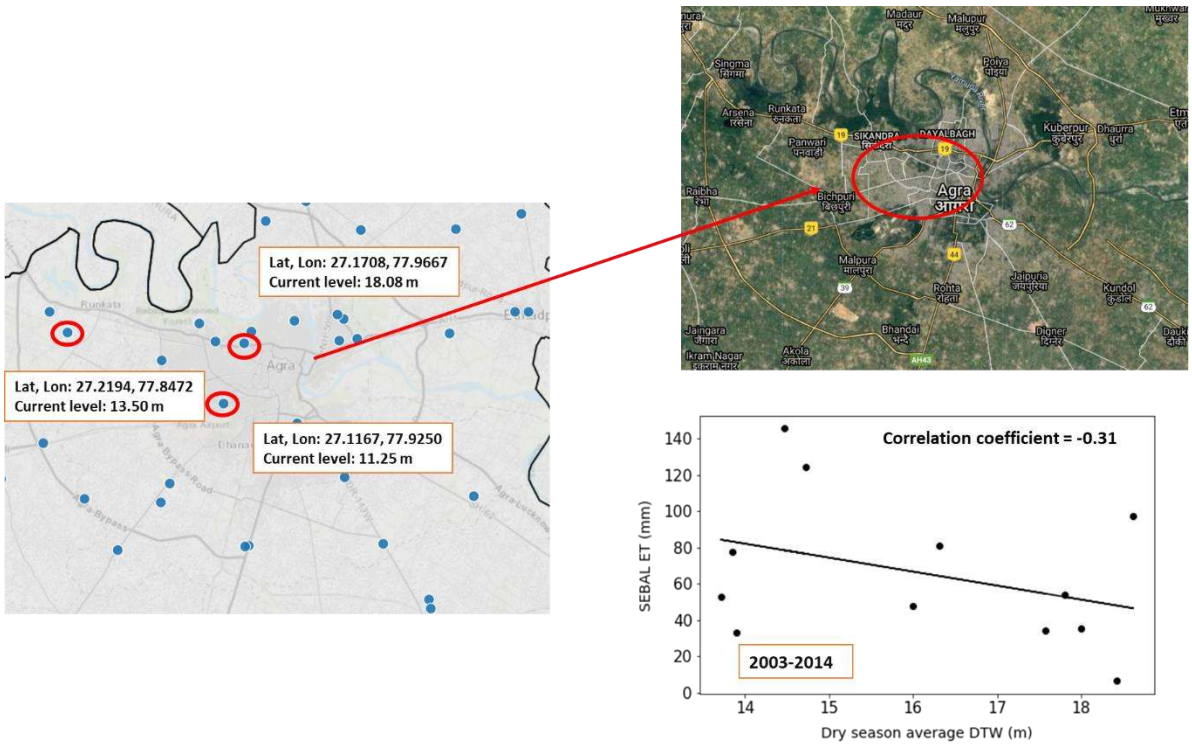

Figure 4.7. Correlation between SEBAL ET and DTW during dry season over control regions (non-cropped) of Agra.

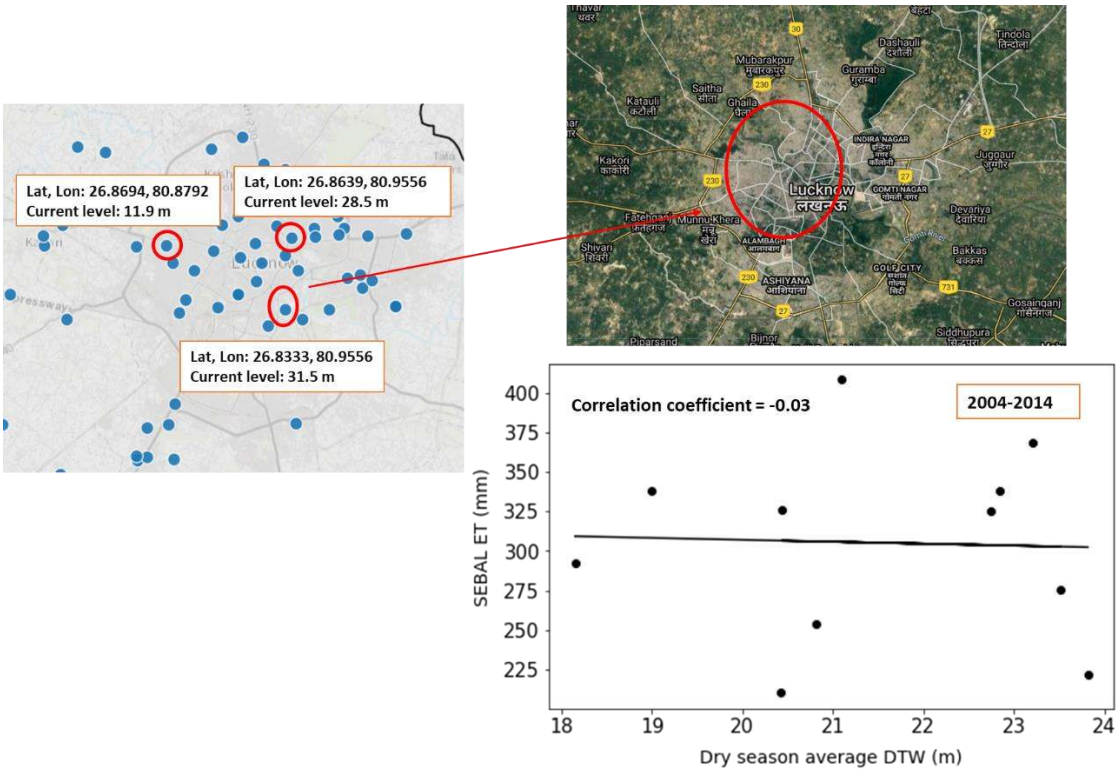

Figure 4.8. Correlation between SEBAL ET and DTW during dry season over control regions (non-cropped) of Lucknow.

4.5 Potential Irrigation Water Savings During Dry Season with IAS

The ultimate goal of this study was to validate if significant amount of water can be saved during dry season using need-based irrigation advisory for the targeted zones identified by GRACE and Landsat TIR data. Hence, we compared the actual water consumption by plants and water required for crop growth and calculated the percentages of over/under irrigation over the selected irrigation districts. The percentages of over-irrigation demonstrated by our results represent the potential savings of groundwater if there was an IAS service in place during dry seasons from 2002 to 2014 in the irrigation districts. The spatial variation of percentages over/under irrigations over those eight irrigation districts are shown in figures 4.9 and 4.10. Different colors in the map, represent

different range of percentages. Red represents the areas with over-irrigation greater than 100% (severe over-irrigation). The orange, yellow, and green colors indicate the areas with over-irrigation varying between 50-100% (moderate over-irrigation), 0-50% (mild over-irrigation) and less than 0% (under irrigation), respectively. We observed that there are extensive areas within each irrigation district that are suffering from severe or moderate over-irrigation.

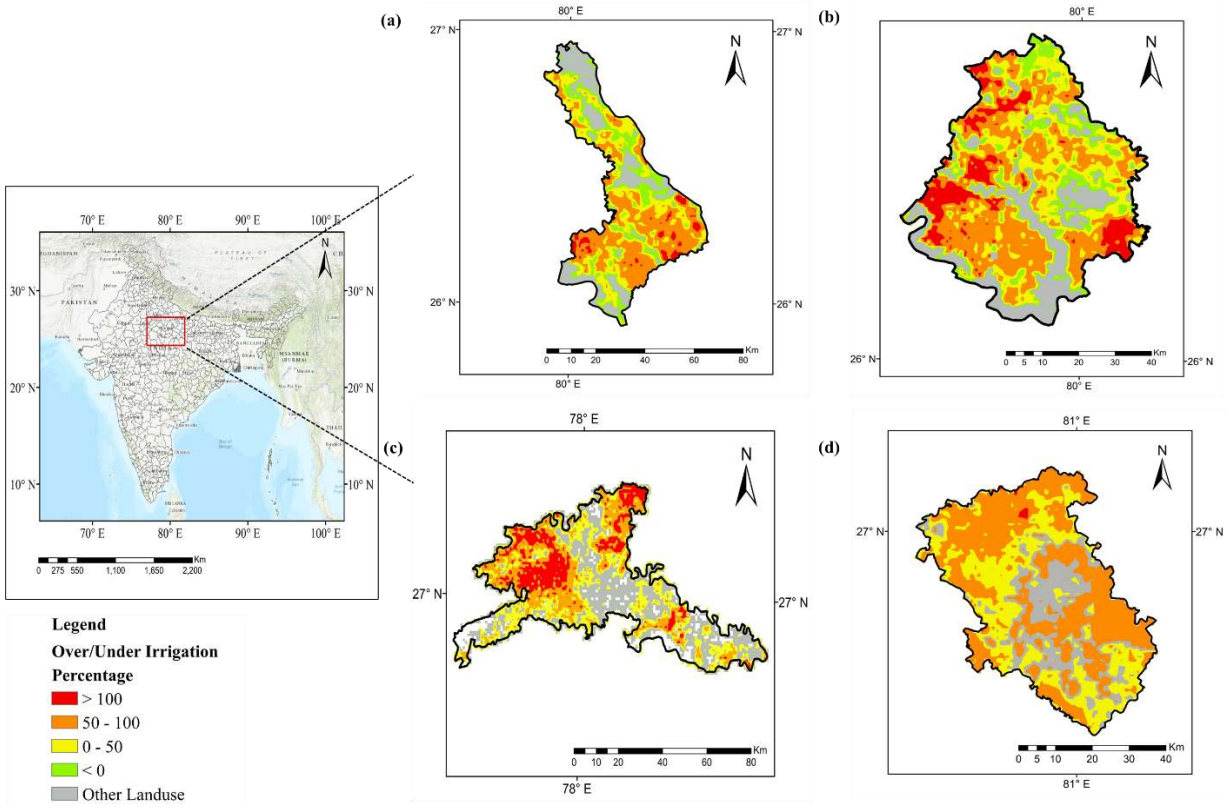

Figure 4.9. Spatial variation of over/under irrigation (January 2013) over (a) Kanpur Nagar, (b) Kanpur Dehat, (c) Agra, and (d) Lucknow in India. Colors showing red, orange, yellow, and green represent percentages greater than 100 (severe over-irrigation), 50-100 (moderate over-irrigation), 0-50 (mild over-irrigation), less than 0 (under irrigation), respectively. Grey color represents the uncropped areas. The scale of the data used is 60 m X 60 m from Landsat TIR bands.

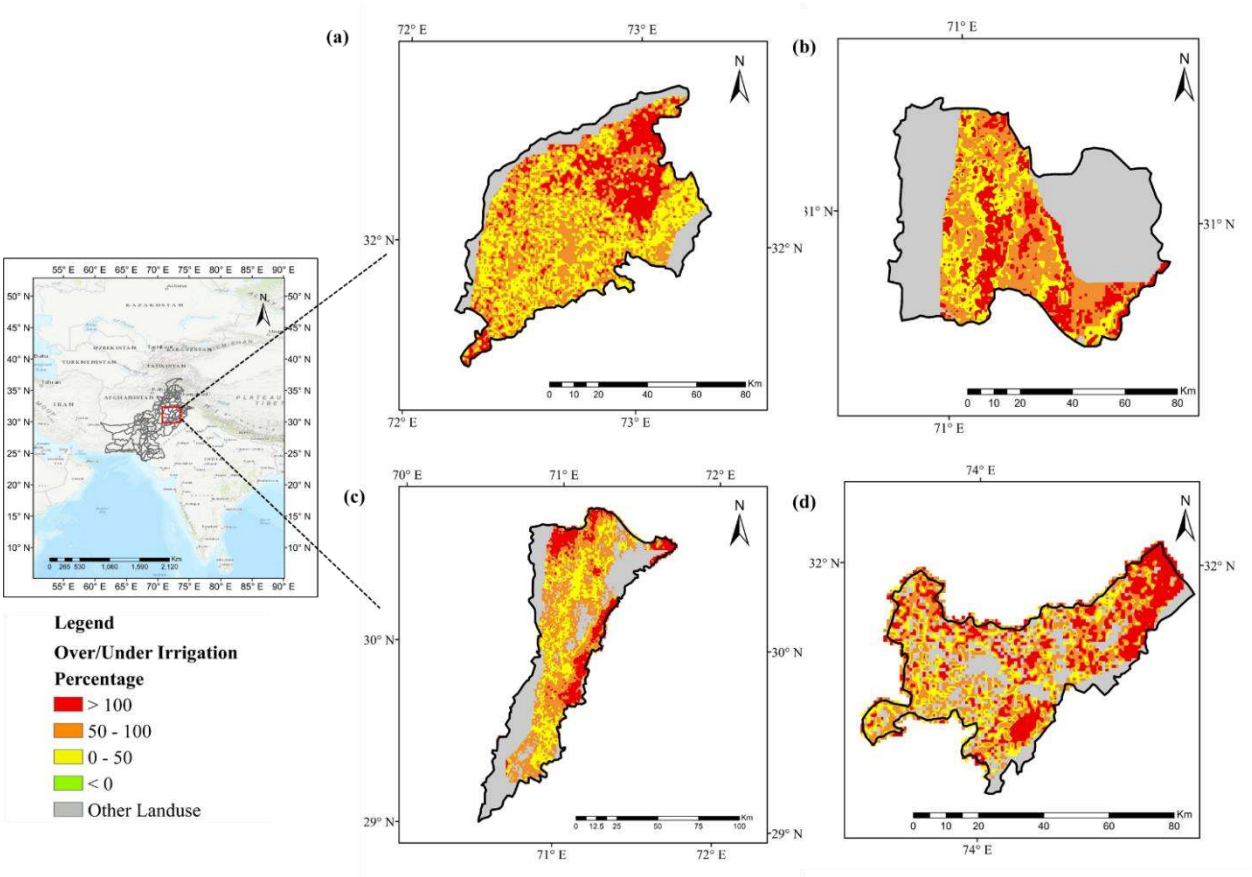

Figure 4.10. Spatial variation of over/under irrigation (January 2013) over (a) Sargodha, (b) Layyah, (c) Muzaffargarh, and (d) Sheikhupura in Pakistan. Colors showing red, orange, yellow, and green represent percentages greater than 100 (severe over-irrigation), 50-100 (moderate over-irrigation), 0-50 (mild over-irrigation), less than 0 (under irrigation), respectively. Grey color represents the uncropped areas. The scale of the data used is 60 m X 60 m from Landsat TIR bands.

Next, we summarized our multi-year analysis of ET data to understand the pattern of average irrigation scenario for each month of the growing season during the dry season (figures 4.11 and 4.12). The results suggested a similar pattern of over-irrigation over the selected districts. The higher percentages of over-irrigation (median and 75th percentile greater than 100) associated with wheat were observed at the beginning of dry season (November, December and, January) with maximum variability and then again in April. For instance, in figure 4.11 (a), for Indian irrigation

districts, the median value during November is approximately 150% and the variability of 25th and 75th percentiles are around 130% and 170%, respectively. The medians and variabilities are much lower during February and March (below 100%). The median value (~80%) and variabilities of 25th and 75th percentiles (~30% to 150%) again increased during April. All other districts showed similar patterns, with expected variabilities due to variation in soil type, soil moisture condition, weather conditions and farmers' irrigation practice.

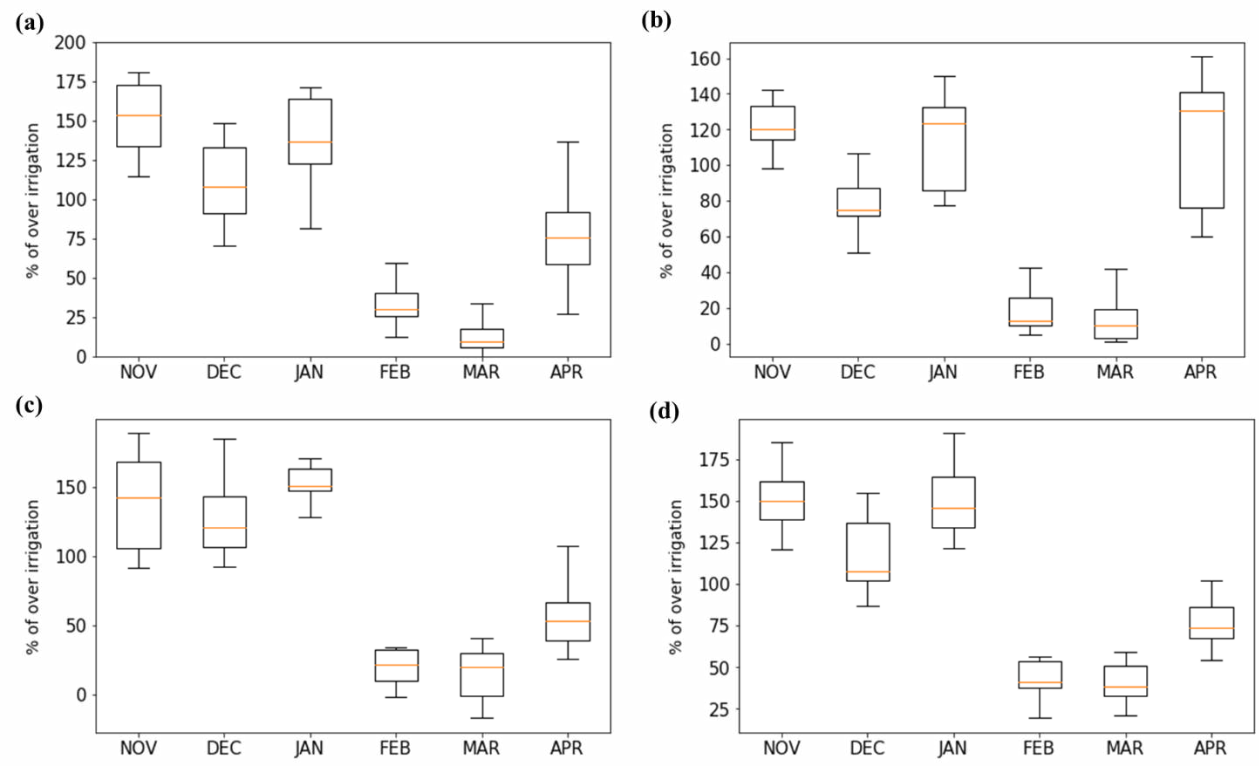

Figure 4.11. Percentages of over-irrigation (considering wheat) during dry season over (a) Kanpur Nagar, (b) Kanpur Dehat, (c) Agra, and (d) Lucknow. The orange lines of the boxplots correspond to the median values of percentages of over-irrigation.

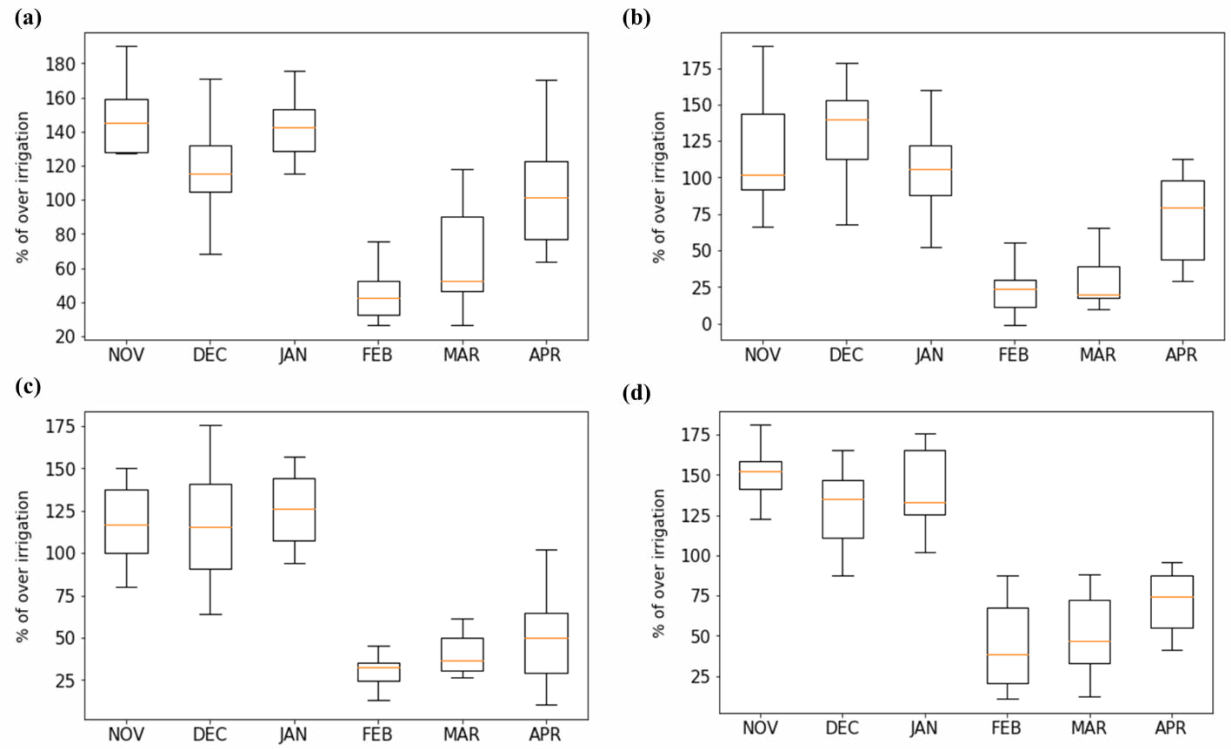

Figure 4.12. Percentages of over-irrigation (considering wheat) during dry season over (a) Sargodha, (b) Layyah, (c) Muzaffargarh, and (d) Sheikhupura. The orange lines of the boxplots correspond to the median values of percentages of over-irrigation.

Given the traditional irrigation practice in South Asia, we are speculating that the higher percentages of over-irrigation at the beginning of dry (winter) season is due to over watering the seeds and young plants or watering more frequently than needed due to the initially-dry soils. Because of this excess/frequent watering, the monthly sum of SEBAL ET (actual water consumption) is higher, which in turn gives us the higher percentage of over-irrigation. In April, as the crop is ready for harvest, a high percentage of over-irrigation may be an effect of some other anticipated effects. For example, there could be an overlap of the rice-growing season that begins in April. In some districts of India there is winter rice that grows simultaneously with wheat and in some districts of Pakistan sugarcane starts growing from April (FAO, 2020). Due to unavailability of high-resolution and time-varying crop maps, we considered only wheat grown all

over the cropped regions on targeted districts. Thus, Penman-Monteith ET provided much smaller values than what it should be, whereas SEBAL ET estimated the actual water consumption. This may potentially result in a high over-irrigation percentage not entirely attributable to the harvested stage of wheat in April. In addition, we assumed Ks = 0.5 for estimating the crop water demand which might be different in the actual scenario based on the soil moisture condition and the pre-monsoon thunderstorms that are common in April. We also estimated SEBAL and Penman-Monteith ETs averaged over the entire cropped regions where plot types, farmer's behavior in decision-making (to irrigate or not to irrigate) may vary and can introduce variability in the estimated percentages in each district.

We evaluated that the multi-year assessment of irrigation corresponded to an average amount of up to 85% (~80 million m^3), 80% (~90 million m^3), 85% (~ 95 million m^3), and 87% (~ 65 million m^3) groundwater that could be potentially saved during dry season over Kanpur Nagar, Kanpur Dehat, Agra, and Lucknow, respectively if farmers followed the IAS advisory. Similarly, an average amount of up to 97% (~160 million m^3), 77% (~140 million m^3), 78% (~ 155 million m^3), and 95% (~ 150 million m^3) groundwater could be potentially saved during dry season over Sargodha, Layyah, Muzaffargarh, and Sheikhupura, respectively. Hence, with an improved IAS, an average amount of 85% (80 million m^3) and 87% (150 million m^3) of groundwater could be saved during a dry season in districts of Northern India and Eastern Pakistan, respectively. It should be noted that this potential saving (> 80%) is much larger than the earlier surveyed savings of 40% of groundwater with the current IAS that does not precision-target regions based on groundwater waste footprint.

4.6 IMPACT EVALUATION OF PCRWR IAS

We further verified the impact of IAS over four irrigation districts of Pakistan, where PCRWR is actively operating IAS since 2016. PCRWR launched the service on April 18, 2016, which is an outcome of international collaboration extended by the University of Washington (UW) and NASA. The UW is providing real time daily Potential Evapotranspiration (ET) and precipitation for entire Pakistan using NASA's remotely sensed data. Starting with 700 farmers in 2016, the service was then expanded to 10,000 farmers of 21 districts of different agro-climatic zones in January 2017. Then it gradually scaled up to 40,000-100,000 farmers and according to a survey of randomly selected farmers carried out by PCRWR, it is speculated that the IAS can potentially save about 2.5 km3 of groundwater a year per 100,000 farmers in Pakistan (IAS, 2018; http://www.pcrwr.gov.pk/advisory.php).

To assess if the implementation of IAS had any quantifiable impact on irrigation water use reduction, we carried out an unbiased sampling experiment. We assumed first that the year of IAS implementation was unknown and therefore needed to be identified forensically. We then tried different implementation years for IAS from 2012 to 2019 and evaluated the difference between the mean of pre-IAS and post-IAS SEBAL ET. We then identified the year that yielded the highest difference in mean SEBAL ET (actual water consumption) between pre-IAS (before the implementation year) and post-IAS (after the implementation year). This would indicate that the mean of pre-IAS actual water consumption was greater than the mean of pre-IAS actual water consumption (figure 4.13). In other words, if 2016 happened to be the year that yielded highest difference between pre-IAS and post-IAS SEBAL ET, then there is strong evidence to believe that IAS played a role in reduction in irrigation water use.

In figure 4.13, the x-axis represents the cut-off year, which refers to the assumed year of IAS service initiation. This cut off year divides the assessment period into pre-IAS and post-IAS periods. For example, cut-off year 2016 to 2017 means, we assume IAS was launched in 2016 and the post IAS period starts from 2016 and onwards. We evaluated the pre period considering the mean of SEBAL ET from 2012 to 2015 and the post period considering the mean of SEBAL ET from 2016 to 2019. The y-axis is the difference between mean SEBAL ET/year of pre and post IAS periods (Pre-IAS minus post-IAS). In figures 4.13 (b) and (c), for Layyah and Muzaffargarh the highest difference between pre and post IAS SEBAL ET has been found while 2016 is considered as first implementation year of IAS. This indicates that the mean water consumption has decreased compared to other years, after IAS has been launched during 2016. For Sargodha (figure 4.13 (a)) the highest difference between pre and post IAS SEBAL ET has been found while 2013 is considered as first implementation year. This difference is of greater magnitude compared to other cut-off years. Hence, this could be the impact of a broader and underlying trend such as drought, lack of GW, failing crop prices etc. But if we disregard 2013 as the implementation year, then the highest difference has been observed during cutoff year 2016-2017. On the other hand, for Sheikhupura (figure 4.13 (d)) the trend is different than other three districts. The difference gradually decreased from cut-off year 2013-2014 to 2018-2019, which may be the reason of farmers' not following the advisory properly.

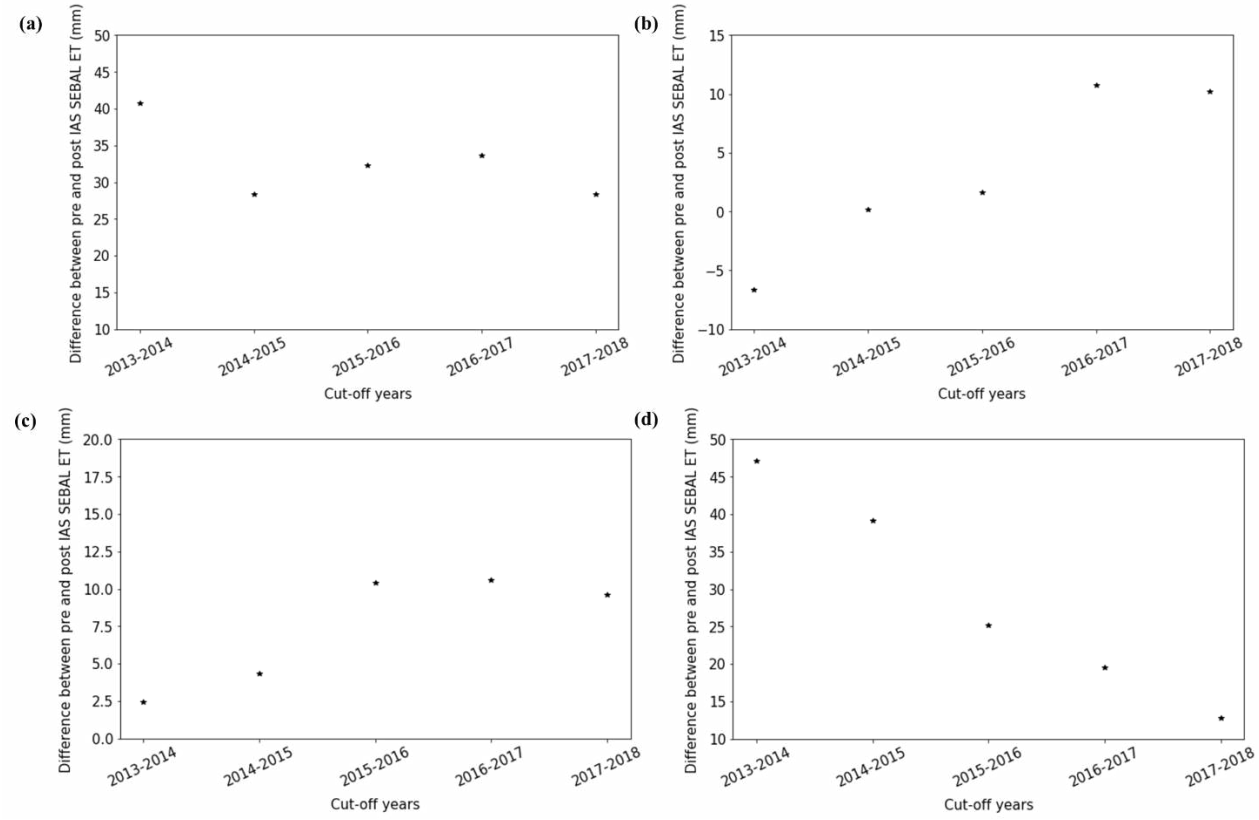

Figure 4.13. Difference between pre and post IAS SEBAL ET considering different start year of IAS over (a) Sargodha, (b) Layyah, (c) Muzaffargarh, and (d) Sheikhupura.

Next, we also observed the spatial variation (figures 4.14 to 4.17) of pre-IAS and post-IAS (considering 2016 to 2017 transition period) mean SEBAL ET over those four districts to spatially find if over any region the average water consumption has increased or decreased. Different colors are referring to different range of SEBAL ETs, where red color is for the highest and dark green color is for the lowest range of ETs. In figures 4.14 to 4.16, for Sargodha, Layyah and Muzaffargarh, the overall spatial variation of greater ET values (red color) has decreased during post-IAS period. We speculate this as a potential indication of farmers' adopting IAS. On the contrary, the spatial variation in figure 4.17 for Sheikhupura illustrates that the variation of ET values is not very different during post-IAS period compared to pre-IAS period. This matches with

the trend of figure 4.13 (d). However, from these results it cannot be conclusively proven that IAS has been solely responsible for reducing over-irrigation at district scale since its inception in 2016. Overall, SEBAL ET data during pre and post-IAS with variable IAS start year provide strong evidence that IAS may have played a strong role in reducing over-irrigation and IAS certainly did not increase over-irrigation in the districts studied when compared with historical water use trend from SEBAL ET.

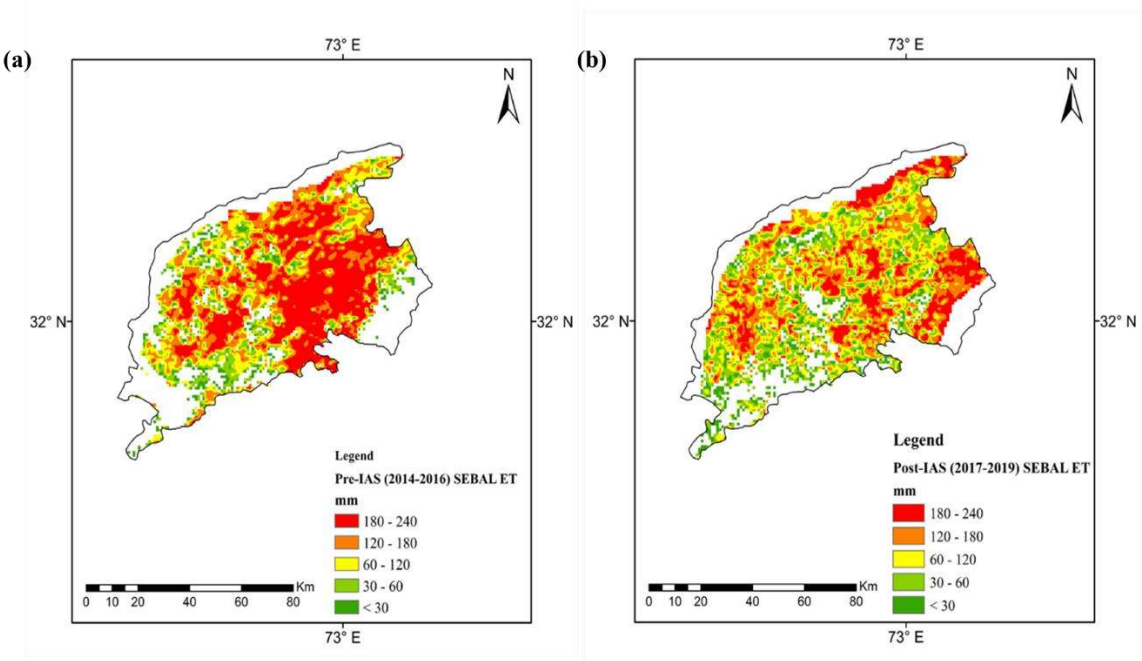

Figure 4.14. (a) Pre-IAS and (b) Post-IAS, spatial variation of mean SEBAL ET over Sargodha considering 2016 as IAS start year.

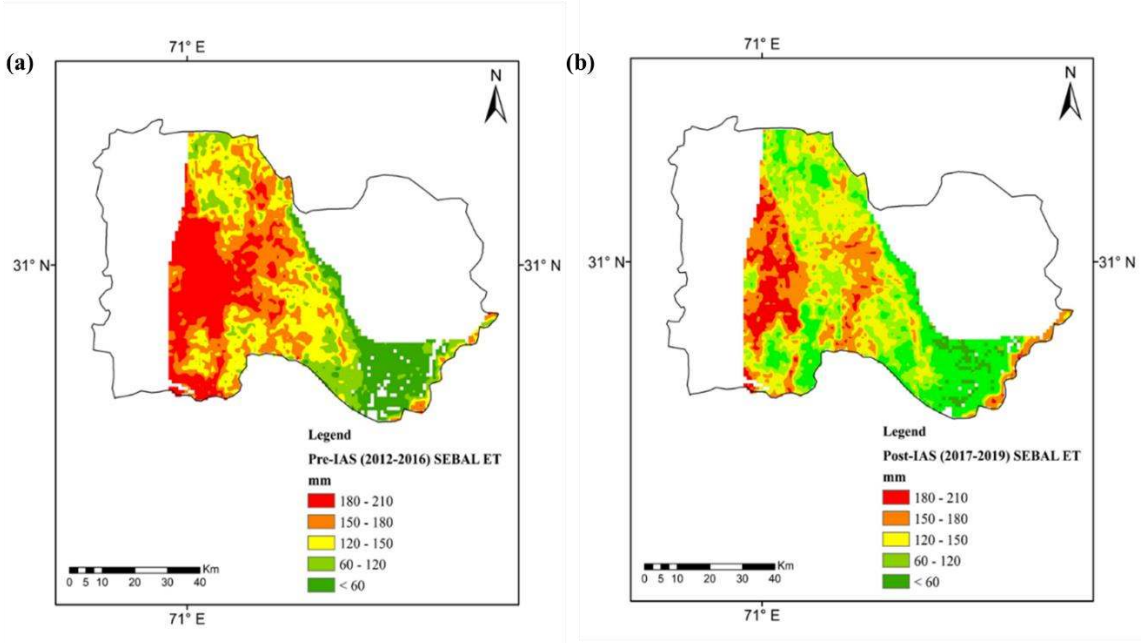

Figure 4.15. (a) Pre-IAS and (b) Post-IAS, spatial variation of mean SEBAL ET over Layyah considering 2016 as IAS start year.

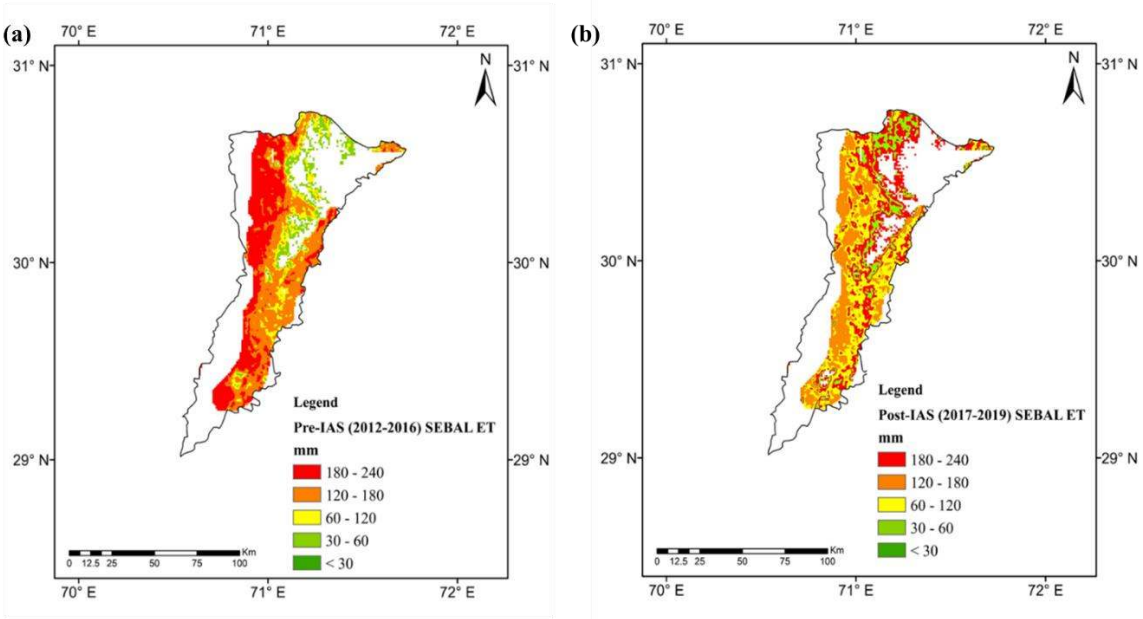

Figure 4.16. (a) Pre-IAS and (b) Post-IAS, spatial variation of mean SEBAL ET over Muzaffargarh considering 2016 as IAS start year.

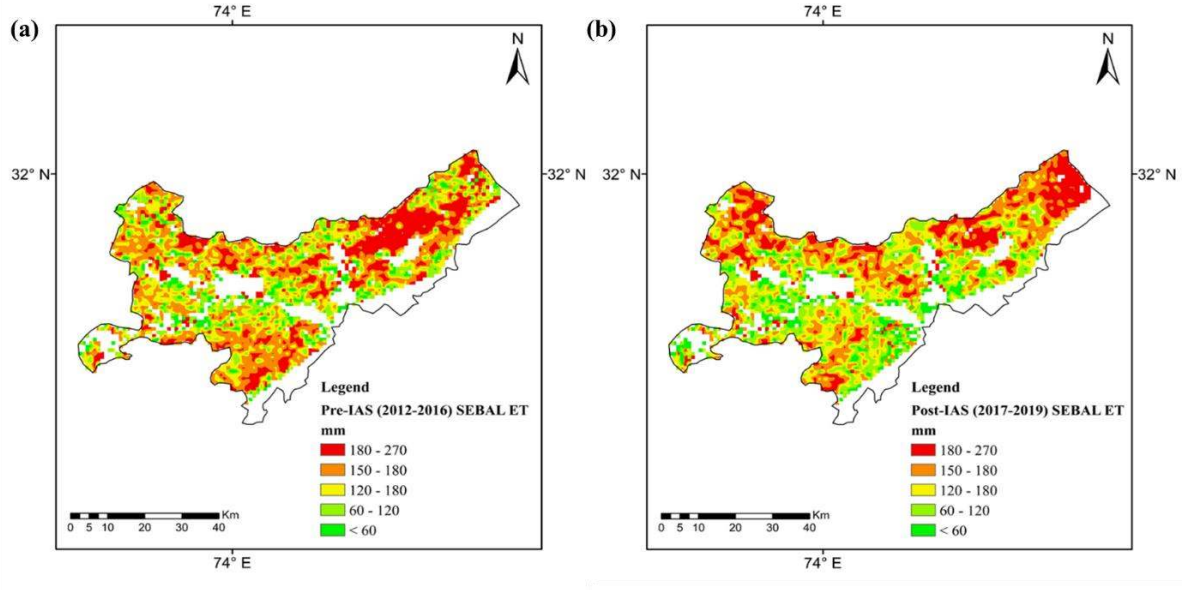

Figure 4.17. (a) Pre-IAS and (b) Post-IAS, spatial variation of mean SEBAL ET over Sheikhupura considering 2016 as IAS start year.

Chapter 5. CONCLUSIONS AND FUTURE WORK

According to our study, the improvement of an existing operational IAS may help reduce the excessive pumping (during dry season) of groundwater in South Asia where agricultural expansion remains a critical threat to groundwater sustainability. Proper use of an improved IAS service that can target in a precise manner the most over-irrigating regions, given the limited bandwidth for outreach, can reduce even further the cost of both fuel for pumping and irrigation advisory texts. In this study, we have argued that an operational IAS can even be more effective if we integrate the GRACE TWS and Landsat TIR data to strategically target regions with more alarming rates of depletion, followed by advising specific farmers and their plots (at scale of 60 m X 60 m) on how much to reduce pumping.

Our results demonstrated the importance of GRACE TWS data to cost-effectively and rapidly identify the most critical regions of unsustainable groundwater decline due to excessive dry season irrigation. The rate of groundwater decline during the dry season may vary from year to year and is difficult to monitor due to lack of in-situ monitoring in South Asia. To maximize the impact of IAS, we focused on a local/district scale and selected eight irrigation districts from Ganges and Indus basins based on the DTW analysis. We compared the relationship of actual water consumption of crops based on SEBAL method with groundwater table data to verify the idea of using GRACE TWS and LANDSAT TIR data in an operational IAS. Strong correlation ranging from 0.71 to 0.79 and 0.75 to 0.87 were found over the Ganges and Indus Basins' districts, respectively. Such consistent correlations provide strong evidence on integration of LANDSAT TIR data to monitor the extent of over-irrigation in an IAS to advise farmers where and when to reduce pumping and stabilize groundwater tables in future.

Advantage of using freely available global satellite observations at high spatial and temporal resolutions makes our proposed improved IAS conceptually transferable to any region in the world where unsustainable dry season irrigation is suspected. Farmers can benefit from such satellite-based precision-targeting IAS by observing how extensive the groundwater waste is when compared to crop water need. The IAS advisory may then encourage farmers to pump less based on crop water needs. Monitoring of SEBAL ET can also help detect behavioral change of farmers in reducing over-irrigation during dry season. Finally, follow up evaluation of GRACE TWS over a larger spatial scale and longer follow-up time period can be explored to understand the effectiveness of an improved IAS that has been in continuous service and whether there is merit in continuing the IAS if there is no tangible impact for national water agencies.

We believe that with such an improved IAS operationalized, the net savings in groundwater can allow the aquifers the necessary breathing space to recharge a little more with each year's monsoon rainfall in South Asia. While doing the analysis, as our first practical trial, we planned to improve the existing IAS in Pakistan with our proposed methodology to save groundwater resources cost effectively and track the long-term impact of this improved IAS. We have already observed in this study that the existing IAS has a positive impact on the districts of Pakistan where IAS is actively operated. Hence, we planned to develop a cloud computing-based tool where GRACE TWS data will be integrated with Landsat TIR in the existing IAS used by PCRWR of Pakistan. This tool will empower PCRWR to find the vulnerable groundwater zones much more rapidly at a scale of 600 km X 600 km (or smaller if necessary). The tool will then help PCRWR zoom in those zones to identify a much higher resolution map on the extent of over-irrigation at the farmer or plot scale using Landsat TIR at 60 m X 60 m. Such a tool will then make it easier for PCRWR to prioritize zones, farmers and plots that need to be sent irrigation advisory given that

only a finite and small fraction of the 4 million farmers of Pakistan can receive such a service today. We hope to report the experience of developing and implementing such a tool for prime time use by a stakeholder in a forthcoming publication.

The take-home messages that can be derived from this study are summarized as follows:

- With the availability of free global satellite observations, our proposed improved IAS is conceptually transferable to any region in the world where unsustainable dry season irrigation is suspected.
- Proper use of an improved IAS service can reduce the cost of advisory texts as well as the cost of fuel for pumping groundwater.
- Improved IAS will find the vulnerable groundwater zones much more rapidly at a scale of 600 km X 600 km (or smaller if necessary) and assess over-irrigation at the farmer or plot scale using Landsat TIR at 60 m X 60 m.
- Enhanced operational IAS may help reduce dry season excessive pumping of groundwater in South Asia. As per our demonstration, the reduction could be about 85% (80 Million m^3) and about 87% (150 Million m^3) of groundwater in an irrigation district in Northern India and Pakistan, respectively.
- Pakistan is expected to be the first beneficiary of this enhanced IAS which will help PCRWR to prioritize zones, farmers and plots that are most vulnerable due to intense groundwater abstraction.
- Enhanced IAS is more impactful over small region/field and crop specific. Hence, high resolution crop maps are needed; soil moisture condition and well data are desired.

At the time of writing the thesis, PCRWR IAS has already been enhanced with GRACE-TIR based IAS service and we are expecting further stakeholder input for revision. The pilot website can be accessed here: https://climateclass.users.earthengine.app/view/smart-irrigation. Our work has also inspired Bangladesh Department of Agricultural Extension and Bangladesh Water Development Board (BWDB) to engage with us for a more enhanced irrigation advisory for North-East Rice farmers in haor regions. We are developing the enhanced IAS tool for North-East region of Bangladesh as well. These are all real-world implementations that our research has enabled, and the impacts can be seen hopefully from 2021.

BIBLIOGRAPHY

Allen, R.G., Pereira, L.S., Raes, D., Smith, M., 1998. Crop evapotranspiration-Guidelines for computing crop water requirements-FAO Irrigation and drainage paper 56. Fao Rome 300, D05109.

Bastiaanssen, W.G., Menenti, M., Feddes, R.A., Holtslag, A.A.M., 1998a. A remote sensing surface energy balance algorithm for land (SEBAL). 1. Formulation. J. Hydrol. 212, 198–212.

Bastiaanssen, W. G., Pelgrum, H., Wang, J., Ma, Y., Moreno, J. F., Roerink, G. J., & Van der Wal, T. 1998b. A remote sensing surface energy balance algorithm for land (SEBAL).: Part 2: Validation. *Journal of hydrology*, *212*, 213-229.

Bhanja, S.N., Mukherjee, A., Rodell, M., 2020. Groundwater storage change detection from in situ and GRACE-based estimates in major river basins across India. Hydrol. Sci. J. 65, 650–659.

Car, N.J., Christen, E.W., Hornbuckle, J.W., Moore, G.A., 2012. Using a mobile phone Short Messaging Service (SMS) for irrigation scheduling in Australia–Farmers' participation and utility evaluation. Comput. Electron. Agric. 84, 132–143.

Castellazzi, P., Longuevergne, L., Martel, R., Rivera, A., Brouard, C., Chaussard, E., 2018. Quantitative mapping of groundwater depletion at the water management scale using a combined GRACE/InSAR approach. Remote Sens. Environ. 205, 408–418.

Castellazzi, P., Martel, R., Rivera, A., Huang, J., Pavlic, G., Calderhead, A.I., Chaussard, E., Garfias, J., Salas, J., 2016. Groundwater depletion in Central Mexico: Use of GRACE and InSAR to support water resources management. Water Resour. Res. 52, 5985–6003.

Chander, G., Markham, B. L., & Helder, D. L. 2009. Summary of current radiometric calibration coefficients for Landsat MSS, TM, ETM+, and EO-1 ALI sensors. *Remote sensing of environment, 113(5),* 893-903.

Corcoles, J.I., Frizzone, J.A., Lima, S., Mateos, L., Neale, C.M.U., Snyder, R.L., Souza, F., 2016. Irrigation advisory service and performance indicators in Baixo Acaraú Irrigation District, Brazil. Irrig. Drain. 65, 61–72.

Dixon, J., Gulliver, A., Gibbon, D. 2001. Farming Systems and Poverty: IMPROVING FARMERS' LIVELIHOODS IN A CHANGING WORLD, FAO and the World Bank. Rome, Italy.

Döll, P., Hoffmann-Dobrev, H., Portmann, F.T., Siebert, S., Eicker, A., Rodell, M., Strassberg, G., Scanlon, B.R., 2012. Impact of water withdrawals from groundwater and surface water on continental water storage variations. J. Geodyn. 59, 143–156.

Earth data, USGS. 2020. Global Food Security Support Analysis Data (GFSAD) Crop Mask 2010 Global 1 km. Retrieved from https://lpdaac.usgs.gov/products/gfsad1kcmv001/. Website accessed on [2020/08/04].

Famiglietti, J.S., 2014. The global groundwater crisis. Nat. Clim. Change 4, 945–948. https://doi.org/10.1038/nclimate2425

FAO (2016). AQUASTAT website. Food and Agriculture Organization of the United Nations (FAO). Website accessed on [2020/08/04].

FAO (2016). AQUASTAT website. Country profile of India. Website accessed on [2020/08/04].

FAO (2016). AQUASTAT website. Country profile of Pakistan. Website accessed on [2020/08/04].

FAO (2020). GIEWS - Global Information and Early Warning System. Website accessed on [2020/08/04].

Fitzpatrick, A., Waite, I. R., D'Arconte, P. J., Meador, M. R., Maupin, M. A., Gurtz, M. E., 1998. Revised Methods for Characterizing Stream Habitat in the National Water-Quality Assessment Program. U.S. GEOLOGICAL SURVEY, Water-Resources Investigations Report 98-4052.

Gao, F., Wang, H., Liu, C., 2020. Long-term assessment of groundwater resources carrying capacity using GRACE data and Budyko model. J. Hydrol. 125042.

Global Forecast System (GFS). (n.d.). Retrieved from: https://www.ncdc.noaa.gov/data access/model- data/model-datasets/global-forcast-system-gfs. Website accessed on [2020/08/04].

Ghaderi, A., Dasineh, M., Shokri, M., Abraham, J., 2020. Estimation of Actual Evapotranspiration Using the Remote Sensing Method and SEBAL Algorithm: A Case Study in Ein Khosh Plain, Iran. Hydrology 7, 36.

Google Earth Engine data Catalog. 2020. Retrieved from: https://developers.google.com/earth-engine/datasets/catalog, Website accessed on [2020/08/04].

Gorelick, N., Hancher, M., Dixon, M., Ilyushchenko, S., Thau, D., Moore, R., 2017. Google Earth Engine: Planetary-scale geospatial analysis for everyone. Remote Sens. Environ., Big Remotely Sensed Data: tools, applications and experiences 202, 18–27. https://doi.org/10.1016/j.rse.2017.06.031

Hossain, F., Biswas, N., Ashraf, M., Bhatti, A.Z., 2017. Growing more with less using cell phones and satellite data. Eos 98.

Hossain, F., Harsha, K. S., Goyal, S., Ahmad, S., Lohani, B., Balaji, N., & Tripathi, S., 2020. Towards Affordable and Sustainable Water-Smart Irrigation Services. AWRA IMPACT, 22, 28-29.

IAS. 2018. Impact Evaluation of PCRWR Irrigation Advisory Service (available online only - www.saswe.net/publications/PakistanImpactEvaluation.pdf)

Irrigation and Weather Advisory System (IWAS) for Pakistan. (n.d.). Website: www.pak-ias.org or http://www.pcrwr.gov.pk/advisory.php). Website accessed on [2020/08/04]

Iqbal, N., Hossain, F., Lee, H., Akhter, G., 2017. Integrated groundwater resource management in Indus Basin using satellite gravimetry and physical modeling tools. Environ. Monit. Assess. 189, 128.

Iqbal, N., Hossain, F., Lee, H., Akhter, G., 2016. Satellite gravimetric estimation of groundwater storage variations over Indus Basin in Pakistan. IEEE J. Sel. Top. Appl. Earth Obs. Remote Sens. 9, 3524–3534.

Li, B., Rodell, M., Kumar, S., Beaudoing, H.K., Getirana, A., Zaitchik, B.F., de Goncalves, L.G., Cossetin, C., Bhanja, S., Mukherjee, A., 2019. Global GRACE data assimilation for groundwater and drought monitoring: Advances and challenges. Water Resour. Res. 55, 7564–7586.

Liang, X., Wood, E. F., & Lettenmaier, D. P. (1996). Surface soil moisture parameterization of the VIC-2L model: Evaluation and modification. Global and Planetary Change, 13(1-4), 195-206.

Liou, Y.-A., Kar, S.K., 2014. Evapotranspiration estimation with remote sensing and various surface energy balance algorithms—A review. Energies 7, 2821–2849.

MacDonald, A.M., Bonsor, H.C., Ahmed, K.M., Burgess, W.G., Basharat, M., Calow, R.C., Dixit, A., Foster, S.S.D., Gopal, K., Lapworth, D.J., 2016. Groundwater quality and depletion in the Indo-Gangetic Basin mapped from in situ observations. Nat. Geosci. 9, 762–766.

Malakar, P., Mukherjee, A., Bhanja, S.N., Saha, D., Ray, R.K., Sarkar, S., Zahid, A., 2020. Importance of spatial and depth-dependent drivers in groundwater level modeling through machine learning. Hydrol. Earth Syst. Sci. Discuss. 1–22.

Mekonnen, D., Siddiqi, A., Ringler, C., 2016. Drivers of groundwater use and technical efficiency of groundwater, canal water, and conjunctive use in Pakistan's Indus Basin Irrigation System. Int. J. Water Resour. Dev. 32, 459–476.

Moderate Resolution Imaging Spectroradiometer (MODIS). n.d. Retrieved from: https://modis.gsfc.nasa.gov/about/ (accessed 8.13.20).

Monteith, J. L., and. Unsworth, M. H. 1990. Principles of Environmental Physics, 2nd ed., Edward Arnold, London.

Mukherjee, A., Saha, D., Harvey, C.F., Taylor, R.G., Ahmed, K.M., Bhanja, S.N., 2015. Groundwater systems of the Indian sub-continent. J. Hydrol. Reg. Stud. 4, 1–14.

Ortega, J.F., De Juan, J.A., Tarjuelo, J.M., 2005. Improving water management: The irrigation advisory service of Castilla-La Mancha (Spain). Agric. Water Manag. 77, 37–58.

Provision of Advisory for Necessary Irrigation (PANI). (n.d.). Website: http://www.i-pani.com. Website accessed on [2020/08/04]

Rahman, A.T.M., Mandal, T., Saha, P., Das, J., 2020. Unsustainable groundwater development for irrigation water management under changing climate in lower Ganga River Basin in India. Groundw. Sustain. Dev. 100449.

Ramage, C. S. (1971). Monsoon Meteorology, Academic Press, London, UK.

Richey, A.S., Thomas, B.F., Lo, M.-H., Reager, J.T., Famiglietti, J.S., Voss, K., Swenson, S., Rodell, M., 2015. Quantifying renewable groundwater stress with GRACE. Water Resour. Res. 51, 5217–5238.

Rodell, M., Famiglietti, J.S., Wiese, D.N., Reager, J.T., Beaudoing, H.K., Landerer, F.W., Lo, M.-H., 2018. Emerging trends in global freshwater availability. Nature 557, 651–659.

Rodell, M., Velicogna, I., Famiglietti, J.S., 2009. Satellite-based estimates of groundwater depletion in India. Nature 460, 999–1002.

Salam, M., Cheema, M.J.M., Zhang, W., Hussain, S., Khan, A., Bilal, M., Arshad, A., Ali, S., Zaman, M.A., 2020. Groundwater storage change estimation using grace satellite data in Indus Basin. Big Data Water Resour. Eng. BDWRE 1, 13–18.

Sarkar, T., Kannaujiya, S., Taloor, A.K., Ray, P.K.C., Chauhan, P., 2020. Integrated study of GRACE data derived interannual groundwater storage variability over water stressed Indian regions. Groundw. Sustain. Dev. 100376.

Segovia-Cardozo, D.A., Rodríguez-Sinobas, L., Zubelzu, S., 2019. Water use efficiency of corn among the irrigation districts across the Duero river basin (Spain): Estimation of local crop coefficients by satellite images. Agric. Water Manag. 212, 241–251.

Senay, G.B., Friedrichs, M., Singh, R.K., Velpuri, N.M., 2016. Evaluating Landsat 8 evapotranspiration for water use mapping in the Colorado River Basin. Remote Sens. Environ. 185, 171–185.

Shah, T., 2007. The groundwater economy of South Asia: an assessment of size, significance and socio-ecological impacts. Agric. Groundw. Revolut. Oppor. Threats Dev. 7–36.

Siddique-E-Akbor, A.H.M., Hossain, F., Sikder, S., Shum, C.K., Tseng, S., Yi, Y., Turk, F.J., Limaye, A., 2014. Satellite precipitation data–driven hydrological modeling for water resources management in the Ganges, Brahmaputra, and Meghna Basins. Earth Interact. 18, 1–25.

Siebert, S., Kummu, M., Porkka, M., Döll, P., Ramankutty, N., Scanlon, B.R., 2015. A global data set of the extent of irrigated land from 1900 to 2005. Hydrol. Earth Syst. Sci. 19, 1521–1545. https://doi.org/10.5194/hess-19-1521-2015

Smith, M & Munoz, G, 2002. Irrigation advisory services for effective water use: a review of experiences. Workshop organized by FAO-ICID, Canada.

Tang, Q., Peterson, S., Cuenca, R.H., Hagimoto, Y., Lettenmaier, D.P., 2009. Satellite-based near-real-time estimation of irrigated crop water consumption. J. Geophys. Res. Atmospheres 114.

Taylor, R.G., Scanlon, B., Döll, P., Rodell, M., van Beek, R., Wada, Y., Longuevergne, L., Leblanc, M., Famiglietti, J.S., Edmunds, M., Konikow, L., Green, T.R., Chen, J., Taniguchi, M., Bierkens, M.F.P., MacDonald, A., Fan, Y., Maxwell, R.M., Yechieli, Y., Gurdak, J.J., Allen, D.M., Shamsudduha, M., Hiscock, K., Yeh, P.J.-F., Holman, I., Treidel, H., 2013. Ground water and climate change. Nat. Clim. Change 3, 322–329. https://doi.org/10.1038/nclimate1744

USAID Agrilinks. 2020. Improving Irrigation Services for Marginal Farmers in India. Retrieved from: https://www.agrilinks.org/post/improving-irrigation-services-marginal-farmers-india. Website accessed on [2020/08/04]

Voss, K.A., Famiglietti, J.S., Lo, M., De Linage, C., Rodell, M., Swenson, S.C., 2013. Groundwater depletion in the Middle East from GRACE with implications for transboundary water management in the Tigris-Euphrates-Western Iran region. Water Resour. Res. 49, 904–914.

Water, R., Allen, R., Tasumi, M., Trezza, R., Bastiaanssen, W.G., 2002. Surface Energy Balance Algorithm For Land (SEBAL) advanced training and user manual.

Water Resources Information System of India. (n. d.). Website: https://indiawris.gov.in/wris/. Website accessed on [2020/08/04]

Wood, E.F., Lettenmaier, D.P., 1996. Surface soil moisture parameterization of the VIC-2L model: Evaluation and modifications. Glob. Planet Change 13, 195–206.

APPENDIX A. SCRIPTS USED FOR IMPROVING IAS

The scripts used for GRACE data processing, SEBAL ET, Penman-Monteith ET, percent of over/under irrigation calculation are provided in the github link that can be accessed here: https://github.com/indirabose/Improved-Irrigation-Advisory-System-IAS-.git.

GRACE TWS Anomaly data processing:

Following the steps bellow, GRACE TWS anomaly data can be processed for any region across the world:

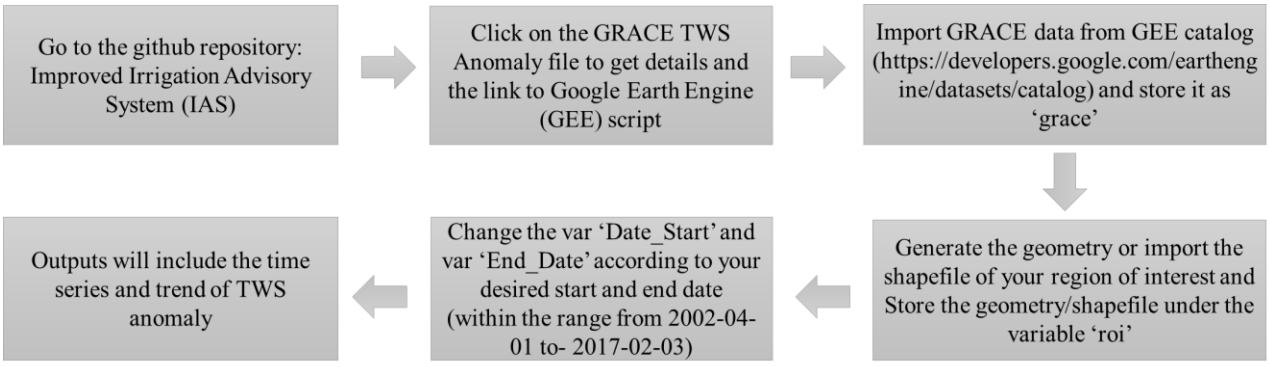

Figure A.1. Steps involved in processing GRACE data and getting TWS anomaly time series and trend using existing scripts over any region across the world.

SEBAL and Penman-Monteith ET processing:

Following the steps bellow, SEBAL and Penman-Monteith ETs can be calculated. The processing of Landsat and GLDAS data is also incorporated in the existing script.

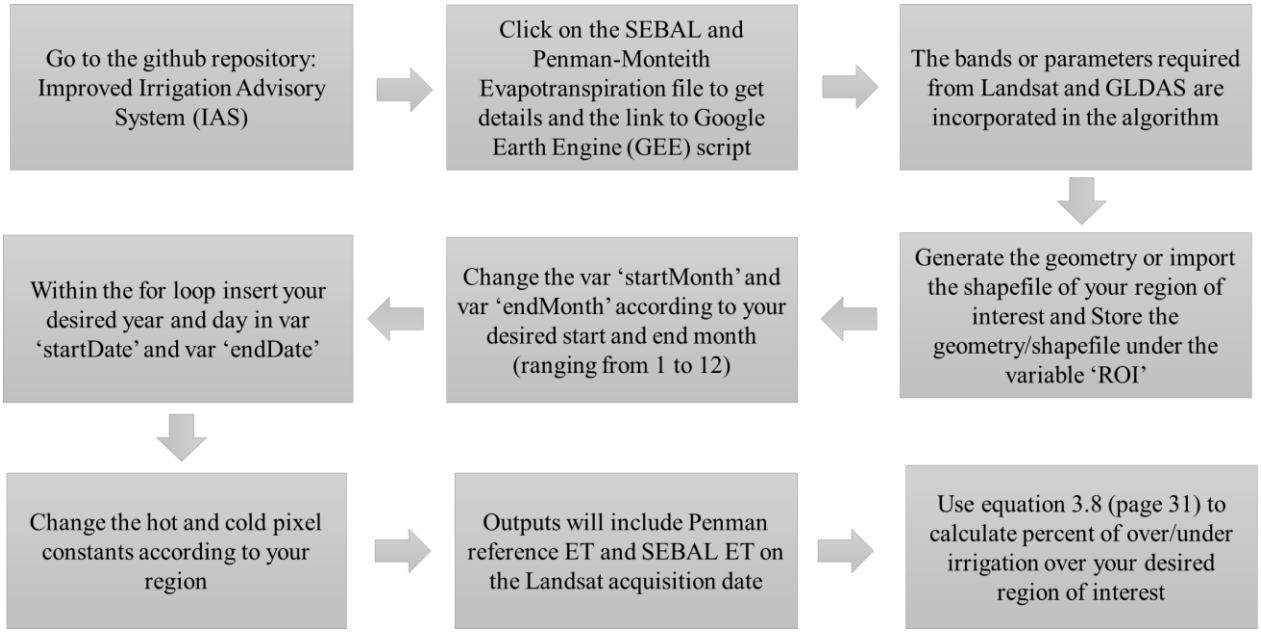

Figure A.2. Steps involved in getting SEBAL and Penman-Monteith ETs using existing scripts over any region across the world.